



HAL
open science

The Polyketide Synthase Pks13 Catalyzes a Novel Mechanism of Lipid Transfer in Mycobacteria

Sabine Gavalda, Fabienne Bardou, Françoise Laval, Cécile Bon, Wladimir Malaga, Christian Chalut, Christophe Guilhot, Lionel Mourey, Mamadou Daffé, Annaïk Quémard

► **To cite this version:**

Sabine Gavalda, Fabienne Bardou, Françoise Laval, Cécile Bon, Wladimir Malaga, et al.. The Polyketide Synthase Pks13 Catalyzes a Novel Mechanism of Lipid Transfer in Mycobacteria. *Chemistry and Biology*, 2014, 21 (12), pp.1660 - 1669. 10.1016/j.chembiol.2014.10.011 . hal-03002982

HAL Id: hal-03002982

<https://hal.science/hal-03002982v1>

Submitted on 20 Nov 2020

HAL is a multi-disciplinary open access archive for the deposit and dissemination of scientific research documents, whether they are published or not. The documents may come from teaching and research institutions in France or abroad, or from public or private research centers.

L'archive ouverte pluridisciplinaire **HAL**, est destinée au dépôt et à la diffusion de documents scientifiques de niveau recherche, publiés ou non, émanant des établissements d'enseignement et de recherche français ou étrangers, des laboratoires publics ou privés.

The Polyketide Synthase Pks13 Catalyzes a Novel Mechanism of Lipid Transfer in Mycobacteria

Sabine Gavalda,^{1,3,4} Fabienne Bardou,^{1,3,4} Françoise Laval,^{1,3} Cécile Bon,^{2,3} Wladimir Malaga,^{1,3} Christian Chalut,^{1,3} Christophe Guilhot,^{1,3} Lionel Mourey,^{2,3} Mamadou Daffé,^{1,3} and Annaïk Quémard^{1,3,*}

¹Department Tuberculose & Biologie des Infections

²Department Biologie Structurale et Biophysique

CNRS, IPBS (Institut de Pharmacologie et de Biologie Structurale), UMR5089, 205 route de Narbonne, BP64182, 31077 Toulouse, France

³Université de Toulouse, UPS, IPBS, 31077 Toulouse, France

⁴Co-first author

*Correspondence: annaik.quemard@ipbs.fr

<http://dx.doi.org/10.1016/j.chembiol.2014.10.011>

SUMMARY

Mycolate-containing compounds constitute major strategic elements of the protective coat surrounding the tubercle bacillus. We have previously shown that FAAL32-Pks13 polyketide synthase catalyzes the condensation reaction, which produces α -alkyl β -ketoacids, direct precursors of mycolic acids. In contrast to the current biosynthesis model, we show here that Pks13 catalyzes itself the release of the neosynthesized products and demonstrate that this function is carried by its thioesterase-like domain. Most importantly, in agreement with the prediction of a trehalose-binding pocket in its catalytic site, this domain exhibits an acyltransferase activity and transfers Pks13's products onto an acceptor molecule, mainly trehalose, leading to the formation of the trehalose monomycolate precursor. Thus, this work allows elucidation of the hinge step of the mycolate-containing compound biosynthesis pathway. Above all, it highlights a unique mechanism of transfer of polyketide synthase products in mycobacteria, which is distinct from the conventional intervention of the discrete polyketide-associated protein (Pap)-type acyltransferases.

INTRODUCTION

Tuberculosis (TB) represents a major public health problem worldwide. This disease remains today one of the leading causes of death from an infectious agent. Nearly nine million people fell ill and 1.3 million died from TB in 2012 (WHO, 2013). Drug-sensitive TB can be cured with a standard 6-month therapy. However, the emergence of multidrug-resistant and extensively drug-resistant *Mycobacterium tuberculosis* strains has challenged TB control. Therefore, the discovery of novel pharmacological targets for the development of a new generation of drugs is urgently needed.

The very thick envelope of *Mycobacterium tuberculosis* and other pathogenic mycobacteria is characterized by a broad array of exotic complex lipids that are key players in the infectious process (Daffé et al., 2014; Jackson et al., 2007). Mycolic acids are α -branched and β -hydroxylated fatty acids of exceptional chain length (e.g., C₆₀-C₉₀ in *Mycobacterium*, C₂₂-C₃₆ in *Corynebacterium*) that typify the *Corynebacteriales* order (Marrakchi et al., 2014). They constitute the major components of the outer membrane (mycomembrane) and are therefore determining factors in the permeability of the envelope (Gebhardt et al., 2007). The vast majority of the mycolic acids esterify the pentaarabinosyl ends of the arabinogalactan forming the cell wall mycolyl-arabinogalactan-peptidoglycan (mAGP) complex. The latter would bind to the human natural killer (NK) cell natural cytotoxicity receptor NKp44, playing a potential role in maintaining NK cell activation (Esin et al., 2013). The remaining mycolic acids form the mycolate-containing lipids composed of one or two mycolyl chains linked to the 6 and 6' positions of trehalose and more scarcely to glucose or glycerol. These lipids constitute major determinants of the pathologies caused by the mycobacteria, acting either as proinflammatory agents, like trehalose dimycolate (TDM) and trehalose monomycolate (TMM) (Geisel et al., 2005; Glickman, 2008), or as T cell activators via their presentation by CD1b protein, like glucose monomycolate (GMM) and glycerol monomycolate (GroMM) (Layre et al., 2009; Moody et al., 2002).

Given the significance of the mycolate-containing compounds in the dialog between the tubercle bacillus and the infected host, the identification of the different biosynthesis steps leading to their formation is a very important issue, especially for the search of novel TB drug targets. Their biosynthesis pathway ends up with the transfer of the mycolyl chains from TMM onto a polyol core (arabinogalactan, trehalose, glucose, and possibly glycerol) by the Ag85ABC mycolyl transferase complex (Belisle et al., 1997; Jackson et al., 1999). Beforehand, the mycolyl chains are produced by a mixed fatty acid synthase (FAS)-polyketide synthase (PKS) biosynthesis pathway, whose pivotal step is catalyzed by the FAAL32-Pks13 system (Gavalda et al., 2009; Léger et al., 2009). The discrete fatty acyl-AMP ligase FAAL32 (or FadD32) activates very long (C₁₆-C₆₀) fatty acyl chains, the "meromycolyl chains," into AMP derivatives and loads them onto

Pks13 enzyme (Léger et al., 2009). The latter is a unique PKS that uses exceptionally long (C₁₆-C₂₆) extender units it condenses to the meromycolyl chains, forming α -alkyl β -ketoesters, the direct precursors of mycolic acids (see Figure S1 available online). We have deciphered the different reaction steps catalyzed by Pks13 (Gavalda et al., 2009; Léger et al., 2009). However, the mechanism of release of its products as well as the subsequent steps leading to the formation of TMM remain unknown. The acyl carrier protein (ACP) domains of the PKSs are activated by a phosphopantetheinyl (P-pant) arm that carries the growing acyl chains (e.g., Figure S1) (Walsh et al., 1997). Upon reaching its full length, the polyketide is generally released from the enzyme by the action of a thioesterase (TE) domain found at the C terminus, typically via a hydrolysis mechanism (in the case of linear molecules) or via a macrocyclisation (Hertweck, 2009). Given the high hydrophobicity of Pks13's products, the current model proposes that they would not be released as free acids in the bacterium by Pks13's own putative TE (TE_{Pks13}) domain but transferred via a discrete unknown acyltransferase (a mycoloyl transferase) onto a hydrophilic acceptor unit (Takayama et al., 2005) (Figure S1). Thus, the TE_{Pks13} domain might have a distinct role, like the function of "proofreading" generally accomplished by an external type II thioesterase (Koglin and Walsh, 2009).

The present work investigates the process of release of mycolic acid precursors from Pks13 enzyme and reveals a mechanism of transfer of PKS products during the formation of complex lipids in mycobacteria. Thus, it allows elucidation of long-sought missing pieces of the mycolate-containing compound biosynthesis pathway.

RESULTS

Pks13 Generates Polyol Derivatives

To characterize the step of release of mycolic acid precursors from Pks13, we had to perform in vitro experiments using the purified enzyme. Indeed, besides the fact that Pks13 is essential for the mycobacterial survival (Portevin et al., 2004), the blockage of one step within mycolic acid biosynthesis has proven to inactivate the complete biosynthesis pathway in the past (Vilchère et al., 2000). For solubility and availability reasons, the condensation assays were run in the presence of the substrates naturally used by *Corynebacterium* Pks13, a radiolabeled myristic acid ([1-¹⁴C]C₁₄ acid) and a chemically synthesized C₁₆ carboxy-acyl-CoA (carboxy-C₁₆-CoA), rather than the longer substrates found in *Mycobacterium*. The mycobacterial Pks13 enzyme was shown to be able to use these short substrates in a recombinant *Corynebacterium* strain to synthesize mycolic acids in vivo (Gavalda et al., 2009). Published data have suggested that α,α -D-trehalose or D-glucose play a role in the biosynthesis of mycolic acids (Promé et al., 1974; Puzo et al., 1979; Shimakata et al., 1986), and a more recent report has shown the requirement of trehalose (Tropis et al., 2005). In order to seek for their potential involvement during the condensation reaction catalyzed by Pks13, assays supplemented with these sugars were realized. The intact reaction media were analyzed by thin-layer chromatography (TLC). We observed the glucose- (Figure 1A, spot c) or trehalose-dependent (Figure 1A, spots a and b) production of radiolabeled compounds, which migrated close to the natural GMM, TMM, and TDM standards, respec-

tively. The MALDI-TOF mass spectrometry (MS) analysis of the cold condensation products was very challenging because of the very low quantity of material. Spectra of the compounds obtained in the presence of trehalose and glucose specifically displayed ion peaks expected for the mono- α -alkyl β -ketoacyl trehalose (TMM keto form or "TMMk") and the mono- α -alkyl β -ketoacyl glucose (GMM keto form or "GMMk"), respectively (Figure 1B). MALDI-TOF/TOF MS/MS analyses induced the fragmentation of these molecules and confirmed their identification (Figure S2).

Interestingly, we observed that an additional radiolabeled compound was formed when glycerol was added to the stocks of enzymes used in the condensation assays (Figure 1A, spot d). MALDI-TOF MS analysis revealed the presence of α -alkyl β -ketoacyl glycerol (GroMM keto form or "GroMMk"; Figure 1B). Moreover, in the absence of acceptor molecule in the reaction, the labeling of the most apolar compound increased (Figure 1A, spot e). The purified compound exhibited a behavior similar to that of the long-chain ketone standard during TLC (Figure S3A) and was identified as a C₂₉ long-chain ketone by MALDI-TOF MS with a [M+H]⁺ ion peak at *m/z* 423.35 (expected *m/z* value: 423.46). Such a compound resulted from the spontaneous decarboxylation of free α -alkyl β -ketoacid released from Pks13 by hydrolysis (Figure S3B).

These data altogether demonstrated that Pks13 generates saccharidic derivatives corresponding to trehalose mono- α -alkyl β -ketoester, the direct precursor of TMM, and to glucose mono- α -alkyl β -ketoester but also a nonsaccharidic derivative, namely glycerol mono- α -alkyl β -ketoester. The quantitative variation of condensation products was measured with respect to the initial concentration of acceptor molecule in the reaction. Significant amounts of TMMk were already observed at the lowest trehalose concentrations: 0.07 and 0.7 mM (Figure S4). In a general manner, increasing concentrations of a given acceptor led to a gradual increase of the quantity of the corresponding α -alkyl β -ketoacid derivative formed up to a plateau. In parallel, the labeling of the long-chain ketone deriving from the free α -alkyl β -ketoacid decreased (Figure S4). Thus, the concentration of acceptor unit available in the reaction medium determines the proportions of α -alkyl β -ketoester and α -alkyl β -ketoacid produced by Pks13. To define the preference of the enzyme between the three acceptors, competition experiments were realized. Different pairs of acceptors at equimolar concentrations were mixed in the reaction medium prior to the addition of FAAL32 and Pks13. Data showed that the predilection of Pks13 for the acceptor unit is the following: trehalose, glucose, and glycerol, in decreasing order (Figure 1C).

Pks13 Has a Narrow Acceptor Specificity

In order to establish the nature of the structural determinants that play a role in the recognition by Pks13, a series of natural analogs of glucose and trehalose (Figure 2B) was evaluated as putative acceptors of the condensation products. In the presence of 6-deoxy-D-glucose, which is devoid of hydroxyl group at position 6 where the acylation naturally occurs, no derivative could be detected by TLC (Figure 2A). D-mannose and D-allose, the epimers at positions 2 and 3 of glucose, respectively, could serve as acceptors in vitro (Figure 2A, spots c'' and c'''), although with a lower efficiency than D-glucose (spot c) and, unexpectedly,

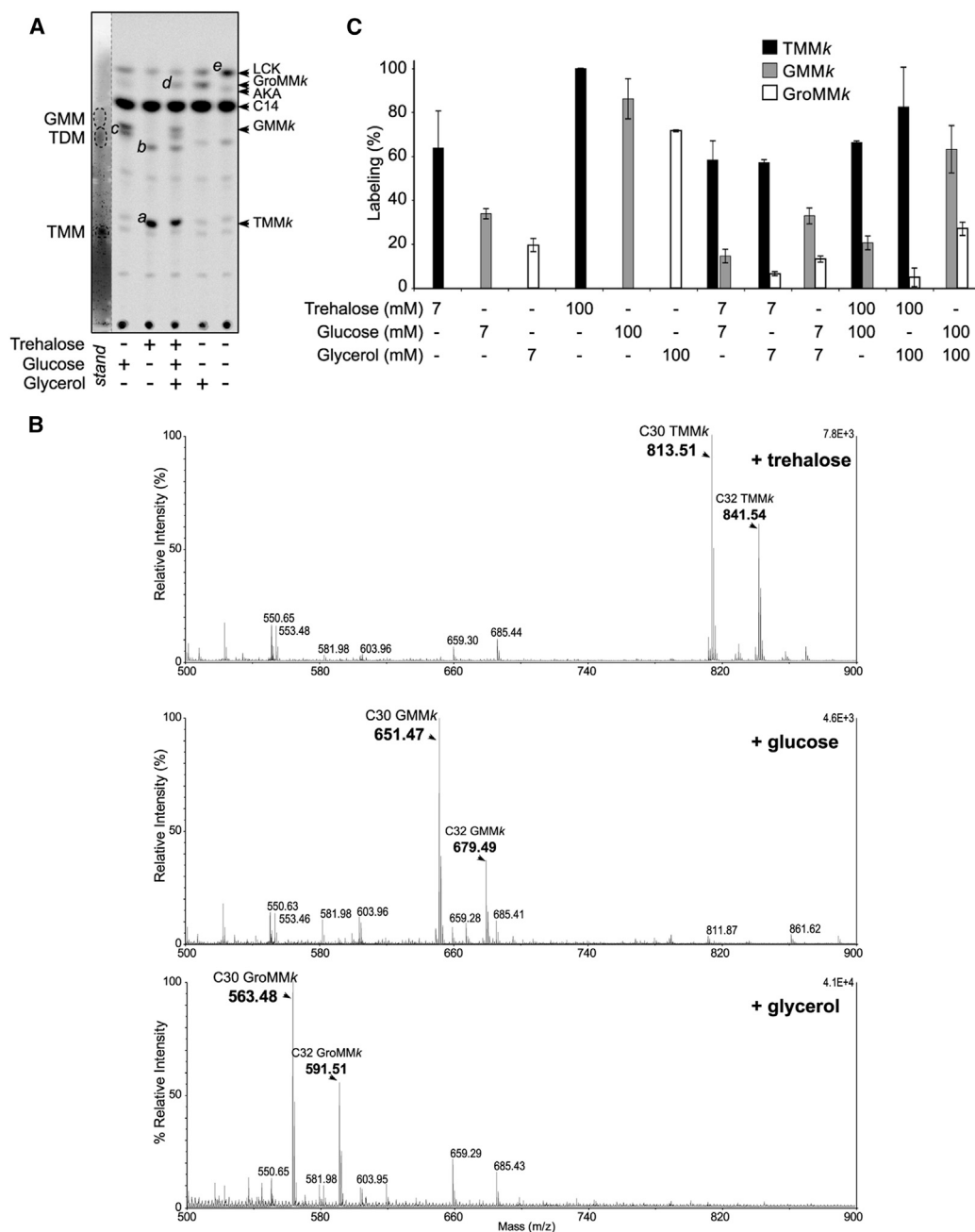


Figure 1. Formation of Different Types of α -alkyl β -ketoacid Derivative by Pks13

(A) TLC/phosphorimaging analysis of condensation assays performed in the absence (–) or in the presence (+) of 50 mM of each putative acceptor. Representative data of three independent experiments. *Stand*, standard mix of TMM, TDM, and GMM (from *C. glutamicum*) revealed by anthrone spraying. Eluent: $\text{CHCl}_3/\text{CH}_3\text{OH}/\text{H}_2\text{O}$, 65/25/4. Spots: a, TMMk; b, palmitoyl TMMk (see note below); c, GMMk (see note in Figure 2 legend); d, GroMMk; e, long-chain ketone (LCK). AKA: α -alkyl β -ketoacid. Note that spot b was identified as (α -myristyl β -ketopalmitoyl),palmitoyl trehalose by MALDI-TOF MS (monosodium adduct at m/z : 1051.75; theoretical m/z value: 1051.76); the C_{16} chain might come from the degradation of an α -alkyl β -ketoacyl chain linked to trehalose by intramolecular retro-Claisen reaction as described previously (Puzo et al., 1979). The minor radiolabeled spots are not linked to the condensation activity.

(B) MALDI-TOF MS analysis of condensation products obtained in the presence of different acceptor molecules. The assays were performed using cold carboxy- C_{16} -CoA, C_{14} acid and 100 mM acceptor molecule. The formation of C_{32} compounds, resulting from the condensation of C_{16} acid and carboxy- C_{16} -CoA, is most likely due to the fortuitous generation of C_{16} acid from carboxy- C_{16} -CoA during the assays. Theoretical m/z values (calculated with the Data Explorer program) of monosodium adducts: C_{30} TMMk, 813.53; C_{32} TMMk, 841.56; C_{30} GMMk, 651.48; C_{32} GMMk, 679.51; C_{30} GroMMk, 563.46; C_{32} GroMMk, 591.50.

(C) Competition experiments between trehalose, glucose, and glycerol as acceptor molecules. The biosynthesis yield of each type of α -alkyl β -ketoacid derivative, in the presence of one or two acceptor molecules at equimolar concentrations, was measured by TLC/phosphorimaging analysis. Data are means of three independent experiments \pm average deviations; they are expressed as relative labelings with the points at 100 mM trehalose arbitrarily set to 100%. See also Figures S2–S4.

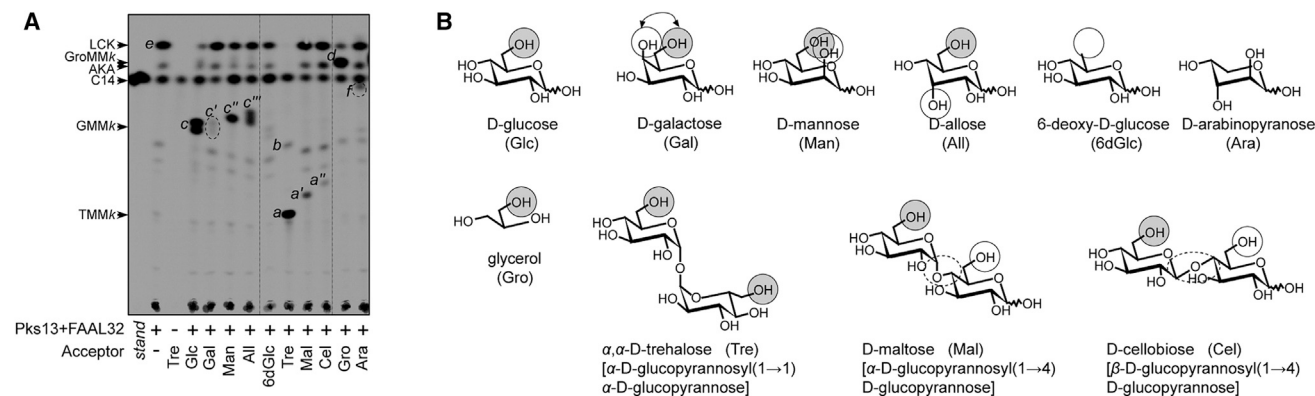


Figure 2. Analogs of Glucose and Trehalose as Putative Acceptors of Pks13's Products

(A) TLC/phosphorimaging analysis of condensation assays performed in the absence (–) or in the presence (+) of 100 mM of putative acceptor. Representative data of three independent experiments. *Stand*, standard [1-¹⁴C]₁₄ acid. Eluent: CHCl₃/CH₃OH/H₂O, 65/25/4. Spots: *a–d* and *f*, mono- α -alkyl β -ketoester of the tested polyol; *e*, long-chain ketone (LCK); AKA, α -alkyl β -ketoacid. Note that the glucose/galactose/allose α -alkyl β -ketoesters appeared as double spots (*c*, *c'*, and *c''*, respectively) most likely because, once released in solution, the neosynthesized α -alkyl β -ketoacyl α -D-monosaccharides isomerize partially into the β tautomers. Indeed, the major forms of the corresponding free sugars in solution are the β -D-glucopyranose tautomers, whereas the mannose, whose α conformation is the major form, generated a single apparent spot (*c''*) of α -alkyl β -ketoester.

(B) Structure of tested compounds.

than glycerol (spot *d*). In the latter, the C–C bonds have no rotation constraint, which allows it to topologically superimpose on half of a glucose molecule (Figure 2B) and may explain its relative success as an acceptor. In contrast, D-galactose, the epimer at position 4 of glucose, was a very bad acceptor (Figure 2A, spot *c'*). These data suggested that the topology of the hydroxyl group at position 4 might dramatically influence the acylation of the hydroxyl group at position 6, probably by steric effect (Figure 2B). In the presence of D-arabinose, the pentose unit found at the extremities of the cell wall arabinogalactan and carrying most of the mycoloyl chains in the outer membrane, a very weak signal was observed (Figure 2A, spot *f*). In the case of disaccharides, the yield of derivative biosynthesis was much lower with D-maltose [Glc(α 1 \rightarrow 4)Glc] (Figure 2A, spot *a'*) than with trehalose [Glc(α , α 1 \rightarrow 1)Glc] (spot *a*), underlining the importance of the nature of the glycosidic bond (Figure 2B). The signal obtained from D-cellobiose [Glc(β 1 \rightarrow 4)Glc] (Figure 2A, spot *a''*) was even weaker than that observed with maltose, showing that a α anomery for the nonreducing glucose unit was favorable to the acyl transfer.

In conclusion, the FAAL32-Pks13 system has a narrow acceptor specificity: both the α -D-glucosyl motif and the (1 \rightarrow 1) link between two glucose units compose the structural bases of an efficient transfer of the neosynthesized α -alkyl β -ketoacyl chains.

Prediction of a Trehalose-Binding Pocket in the TE_{Pks13} Domain

We showed above that the FAAL32-Pks13 system itself catalyzes the release of its products. The fatty acyl-AMP ligase FAAL32 and the acyltransferase domain of Pks13 possess an acyltransferase activity, but they are dedicated to loading the acyl chain of both substrates onto Pks13 (Figure S1) (Gavalda et al., 2009; Léger et al., 2009). We hypothesized that the putative TE domain of Pks13 was responsible for the release step. The TE_{Pks13} domain matched with α/β hydrolases of the

esterase-lipase superfamily, which cleave carboxylic (thio)ester bonds via a nucleophilic attack on the carbonyl. Structure-based sequence comparison of members of this family and programs for model quality evaluation validated the structure of the TE domain of the human fatty acid synthase (TE_{hFAS}) as the best template for homology modeling as well as the good quality of the resulting model (see Supplemental Experimental Procedures). The latter was performed using the structure of TE_{hFAS} in complex with a polyunsaturated fatty acyl substrate analog (Protein Data Bank [PDB] ID 3TJM) (Zhang et al., 2011). The FAS catalyzes the biosynthesis of fatty acids via a Claisen condensation mechanism, a function closely related to that of Pks13. The TE_{Pks13} model displayed a strict conservation of the catalytic triad (Ser1533, Asp1560, His1699 in the TE_{Pks13} domain) (Figure 3A) and of the carboxyl(thio)esterase consensus sequence “G-X-S-X-G” holding the catalytic serine residue (Ser1533) responsible for the nucleophilic attack and the formation of a transient covalent link with the biosynthesis product. Furthermore, superimposition of the TE_{Pks13} model with the TE_{hFAS} structure revealed that the long groove-tunnel that accommodates the fatty acyl chain in TE_{hFAS} domain (Zhang et al., 2011) was also present in TE_{Pks13} model. Interestingly, unlike TE_{hFAS}, the TE_{Pks13} predicted tunnel would open onto a large groove communicating with other grooves and tunnels and might potentially fit a very long fatty acyl chain (Figure S5). Enzymes of the Ag85ABC complex also belong to the α/β hydrolase family and catalyze the transfer of a mycoloyl chain onto a polyol core (the trehalose monomycolate), a function closely related to the mechanism of release of Pks13 products. To seek a putative trehalose-binding site in the TE_{Pks13} domain, the model was compared with the crystal structure of Ag85B-trehalose complex (PDB ID 1F0P) (Anderson et al., 2001). Strikingly, the trehalose-binding pocket near the catalytic site in Ag85B (Figure 3C) superimposed well with a pocket at the bottom of the catalytic cavity in the TE_{Pks13} domain, which might nicely accommodate the disaccharide (Figure 3B). In particular, two residues of Ag85B, the

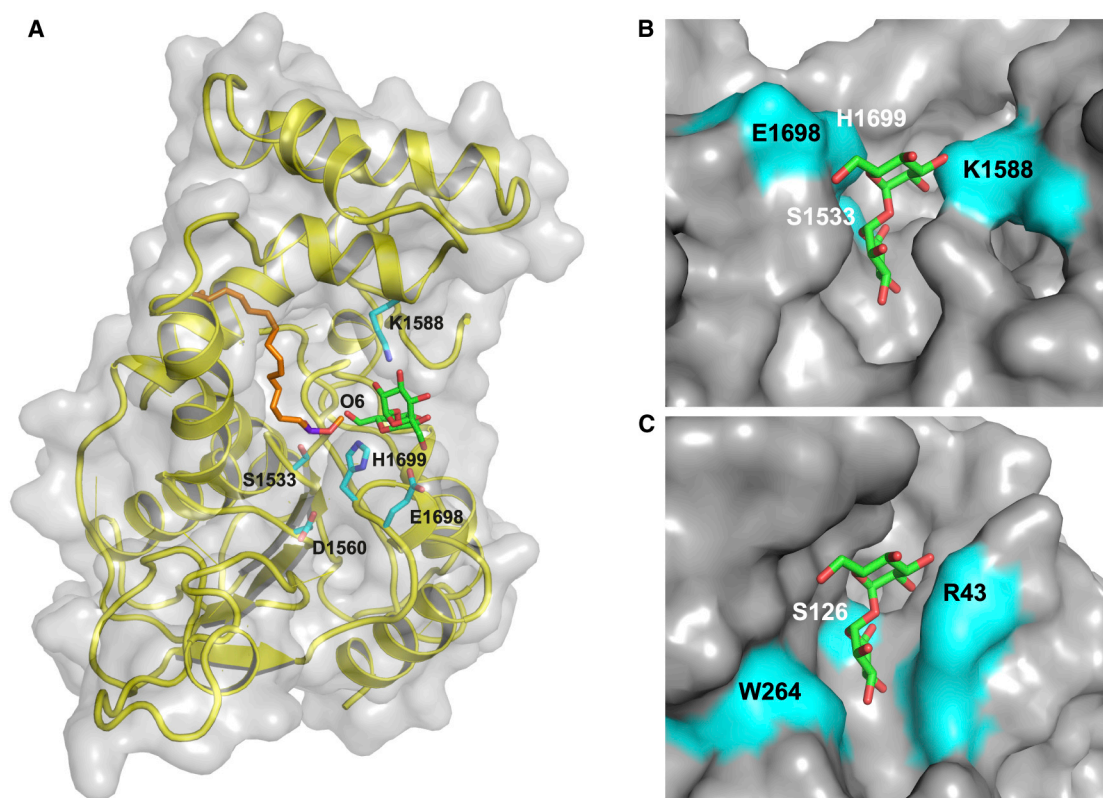


Figure 3. Homology Model of TE_{Pks13} Domain and Its Predicted Trehalose-Binding Pocket

(A) Semi-transparent surface representation of the overall structure with the embedded backbone trace in yellow. The polyunsaturated ligand of the TE_{HFAS} domain, methyl γ -linolenylfluorophosphonate, was positioned by superimposition of the model with the TE_{HFAS} complex structure (PDB ID 3TJM) (Zhang et al., 2011) and drawn as orange sticks. The trehalose ligand of Ag85B enzyme was positioned by superimposition of the model with the Ag85B-trehalose complex structure (PDB ID 1F0P) (Anderson et al., 2001) and colored with carbon atoms in green. Residues of the catalytic triad, Ser1533, Asp1560, and His1699, as well as side chains of additional residues potentially interacting with trehalose (Lys1588 and Glu1698) are colored in cyan. Additional interactions might be mediated via water molecules and protein main chain atoms, as in the Ag85B-trehalose complex (Anderson et al., 2001). N, O, and P atoms are in blue, red, and purple, respectively.

(B) Surface representation of the predicted trehalose-binding pocket in the TE_{Pks13} domain. Residues potentially interacting with trehalose are colored in cyan.

(C) Surface representation of the trehalose-binding pocket in the structure of the Ag85B-trehalose complex. Residues whose side chain directly interacts with trehalose are colored in cyan.

See also Figure S5.

catalytic Ser126 and Arg43, shown to directly interact with trehalose via their side chain, were conserved in the TE_{Pks13} model (Ser1533 and Lys1588, respectively). The side chains of two additional residues of the TE_{Pks13} domain, Glu1698 and the catalytic His1699, might also stabilize a trehalose ligand (Figures 3A and 3B). The hydroxyl group at position 6 of trehalose, where the acylation naturally occurs, would point toward the head group of the fatty acyl ligand, at an adequate distance for a transacylation reaction (Figure 3A).

Taken altogether, these data suggested that the TE_{Pks13} domain was potentially active as a carboxyl(thio)esterase but that it might also be able to welcome a polyol-type molecule in its active site at a proper position for the transfer of an α -alkyl β -ketoacyl chain.

The Isolated TE_{Pks13} Domain Exhibits an Acyltransferase Activity

To experimentally determine the function of TE_{Pks13} domain, we designed an activity assay in the presence of the isolated domain

and of a model substrate, palmitoyl-CoA (C₁₆-CoA), which holds a thioester bond between its acyl chain and the P-part arm of the CoA moiety. We first validated the assay using the whole Pks13 in the presence of [1-¹⁴C]C₁₆-CoA. The release of free C₁₆ acid was strictly dependent upon the presence of Pks13 (Figure 4A, lane 3). In the presence of polyol, additional radiolabeled compounds appeared suggesting the formation of palmitoyl glucose (spot χ), trehalose (spots α and β), and glycerol (spot δ) derivatives (Figure 4A, lanes 4–7). Importantly, the synthesis of palmitic acid or polyol derivatives could not be detected using heat-inactivated Pks13 (Figure 4A, lane 2). Then, the TE_{Pks13} domain was produced and purified to homogeneity from a recombinant *E. coli* strain (Figure S6). Similar to Pks13, incubation of the separate TE domain in the presence of [1-¹⁴C]C₁₆-CoA induced the release of some C₁₆ acid as shown by TLC and MS analysis (Figure 4B, lanes 4 and 7–10; Table S1). It also triggered the formation of additional compounds in the presence of molecules holding an α -D-glucose unit, namely trehalose, glucose, and maltose, as well as in the presence of glycerol (Figure 4B, lanes

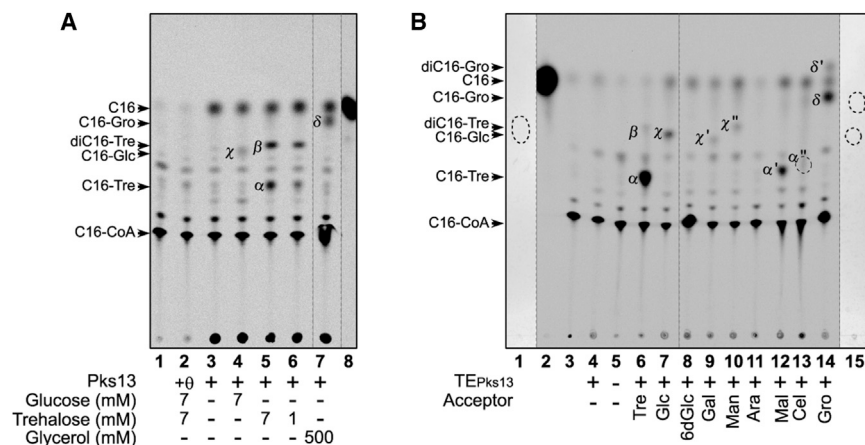


Figure 4. Thioesterase and Acyltransferase Activities of TE_{Pks13} Domain

These activities were measured in the presence of a model substrate, [¹⁴C]C₁₆-CoA, by TLC/phosphorimaging analysis. Representative data of three independent experiments. Eluent: Butan-1-ol/acetic acid/H₂O, 80/25/40. Spots: α, monoalmitoyl trehalose (C₁₆-Tre); α', palmitoyl maltose; α'', palmitoyl cellobiose; β, dipalmitoyl trehalose (diC₁₆-Tre); χ, palmitoyl glucose (C₁₆-Glc); χ', palmitoyl galactose; χ'', palmitoyl mannose; δ, palmitoyl glycerol (C₁₆-Gro); δ', dipalmitoyl glycerol (diC₁₆-Gro).

(A) Validation of the assay using the entire Pks13. Lane 1, [¹⁴C]C₁₆-CoA standard; lanes 2–7, assays in the absence (–) or in the presence (+) of the mentioned putative acceptor molecule (at the indicated concentration); θ, heat-inactivated Pks13; lane 8, [¹⁴C]C₁₆ acid standard.

(B) TE_{Pks13} domain activity assays. Lane 1, diC₁₆-Tre standard; lane 2, [¹⁴C]C₁₆ acid standard; lane 3, [¹⁴C]C₁₆-CoA standard; lanes 4–14, assays in the absence (–) or in the presence (+) of the mentioned putative acceptor molecule (at 100 mM); lane 15, mix of C₁₆-Glc and C₁₆-Gro standards; 6dGlc, 6-deoxy-glucose. Cold standards were visualized by rhodamine B spraying and UV light.

See also Figure S6 and Table S1.

6, 7, 12, and 14). Consistently, MALDI-TOF spectra displayed the signals expected for the palmitoylated derivatives of these polyols (Table S1). In the presence of the other tested molecules (galactose, mannose, 6-deoxy-glucose, arabinose, and cellobiose), the activity of C₁₆ acyl transfer was very weak or undetectable (Figure 4B). Kinetic experiments performed with the TE_{Pks13} domain determined an apparent K_m for trehalose of 5.5 ± 0.1 mM, which was similar to values reported for trehalose-metabolizing enzymes (Kizawa et al., 1995; Riby and Galand, 1985). Consistent with Pks13's substrate specificity, the TE_{Pks13} domain exhibited a marked predilection for trehalose as compared with glucose, with an apparent K_m of 518 ± 30 mM for the latter. The very high K_m value for glucose suggests that trehalose would be the specific acceptor of the neosynthesized α-alkyl β-ketoacyl chains in vivo.

In conclusion, the isolated TE domain of Pks13 is active and is able, like the entire Pks13 enzyme, to catalyze the transfer of a C₁₆ acyl chain from a P-pant arm onto trehalose.

The Transfer of Pks13 Condensation Products Is Catalyzed by Its Own TE Domain

To demonstrate the involvement of the TE domain in the transfer of the neosynthesized α-alkyl β-ketoacyl chains onto a polyol acceptor, the putative catalytic Ser1533 of Pks13 (Figure 3) was mutated into an Ala residue. Condensation assays for both wild-type (WT) Pks13 and Pks13 S1533A were performed in parallel in the presence of both trehalose and glycerol. Analysis of the intact samples revealed the lack of formation of α-alkyl β-ketoacid derivatives (TMMk and GroMMk) by Pks13 S1533A by comparison with WT Pks13 (Figure 5A, lanes 2 and 3). The lipid moiety of the condensation products was analyzed after chemical treatment (Figure 5C). A residual synthesis of condensation products (7%) by the mutant enzyme with respect to WT Pks13 was observed (Figure 5B, lanes 2 and 3). It most likely represented the α-alkyl β-ketoacyl chain that remained blocked on the C-terminal ACP domain (Figure S1) in the absence of an active TE domain. When some of the isolated WT TE_{Pks13} domain

was added to the condensation assay with Pks13 S1533A, the acyltransferase function was recovered since some TMMk and GroMMk were synthesized (Figure 5A, lanes 4 and 5). In this case, the total condensation rate reached 18%–24% (Figure 5B, lanes 4 and 5). Thus, the WT TE_{Pks13} domain was able to partially complement the S1533A mutation in the TE domain of the entire Pks13 enzyme.

These data altogether established that the TE_{Pks13} domain is responsible for both the release and the transfer of Pks13 products onto a polyol acceptor molecule, particularly trehalose, and that S1533 is a key residue for this catalytic process (Figure S7). In the absence of an active TE domain, there is no catalytic turnover.

DISCUSSION

It is known that the ultimate biosynthesis steps of the mycolate-containing compounds are catalyzed by the mycoloyl transferases of the Ag85 complex. The latter transfers the mycoloyl chains from the TMM donor onto an acceptor, mainly arabinogalactan or another TMM but also glucose and possibly glycerol, to form the mAGP complex, TDM, GMM, and GroMM, which will reach their final locations in the mycomembrane (Figure 6) (Belisle et al., 1997; Jackson et al., 1999). However, the steps between the synthesis of the mycoloyl chains and the formation of TMM remained unknown, although they have been the subject of extensive investigations.

The present study allows elucidation of the missing steps and how to draw a scheme of the mycolate-containing compound biosynthesis (Figure 6). We have previously reported that after loading onto Pks13, the meromycolic and carboxyacyl chains are condensed via a Claisen-type mechanism by the ketosynthase domain of Pks13, resulting in an α-alkyl β-ketoacyl chain linked to the C-terminal ACP domain (Gavalda et al., 2009). Here we show that these highly insoluble mycolic acid precursors are not released as free acids in the bacterium by a classical hydrolysis step but are directly transferred onto a hydrophilic

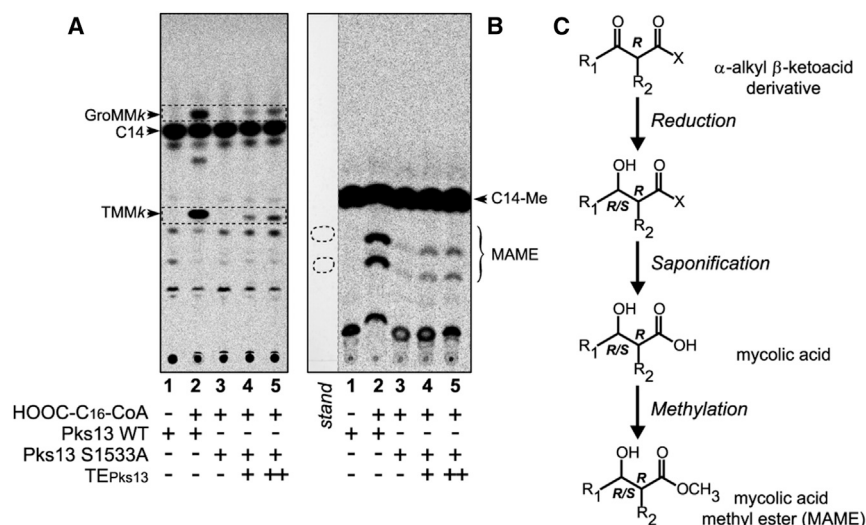


Figure 5. Condensation Assays Using Pks13 S1533A Enzyme

(A and B) TLC/phosphorimaging analyses. Representative data of three independent experiments. All assays were performed in the presence of trehalose and glycerol. Lanes 1, control assay without carboxy-C₁₆-CoA; lanes 2, assay with WT Pks13; lanes 3, assay with Pks13 S1533A; lanes 4, assay with Pks13 S1533A plus TE_{Pks13} domain; lanes 5, similar to lanes 4 with a double concentration of TE_{Pks13} domain (see [Experimental Procedures](#)); stand, cold standard of racemic mixture of C₃₂ mycolic acid methyl esters (MAME), visualized by rhodamine B spraying and UV light.

(A) Intact reaction media. Eluent: CHCl₃/CH₃OH/H₂O, 65/25/4.

(B) Lipid moiety of the condensation products. Eluent: CH₂Cl₂.

(C) Chemical treatment of the condensation products for analysis of their lipid moiety. R₁ = C₁₃, R₂ = C₁₄, X = trehalose or glycerol (in assays 2, 4, and 5 in A and B) or Pks13 S1533A (in assay 3). For details, see [Experimental Procedures](#). See also [Figure S7](#).

head, specifically trehalose ([Figure S7](#)). In conflict with the current biosynthesis model, our data demonstrate that their transfer is not performed by a discrete mycoloyl transferase as proposed earlier ([Besra et al., 1994](#); [Datta and Takayama, 1993](#); [Takayama et al., 2005](#)) but by Pks13's own TE domain. Thus, the latter releases the condensation products from the P-pant arm of the ACP domain, most likely via the formation of a transient ester bond with its catalytic Ser1533 residue ([Figure S7](#); [Figure 6](#)). Then, the TE_{Pks13} domain catalyzes the cleavage of this bond and the concomitant transfer of the α-alkyl β-ketoacyl chain onto trehalose. The previous observations of an accumulation of α-alkyl β-ketoacyl trehalose in *cmrA* mycobacterial mutants deficient in the subsequent mycolic reductase step ([Bhatt et al., 2008](#); [Lea-Smith et al., 2007](#)) are perfectly consistent with our data. After reduction by CmrA, the resulting TMM is translocated via MmpL3 transmembrane protein ([Grzegorzewicz et al., 2012](#); [Tahlan et al., 2012](#); [Varela et al., 2012](#)) toward the Ag85 complex tightly associated to the mycomembrane ([Bou Raad et al., 2010](#); [Marchand et al., 2012](#)). The Ag85 enzymes then use TMM as a substrate for the biosynthesis of the mAGP complex and the mycolate-containing lipids located in the mycomembrane ([Figure 6](#)). LpqY-SugA-SugB-SugC ABC transporter mediates the retrograde transport of the extracellular released trehalose ([Kalscheuer et al., 2010](#)). This recycling step is critical for virulence of *M. tuberculosis* during the acute infection phase, which may be linked to the requirement of trehalose in the construction of the mycolic acid coat ([Kalscheuer et al., 2010](#)).

Similar to the mycolate-containing lipids, the biosynthesis of most lipid pathogenicity factors of the mycobacterial envelope depends upon the intervention of PKSs ([Daffé et al., 2014](#); [Jackson et al., 2007](#)). For such molecules, data clearly outline an archetypal building and translocation pattern where fatty acyl chains are synthesized by specific PKSs, then transferred onto a polyol core, most often trehalose or substituted trehalose, and after potential extra modifications, the product is ultimately exported toward the envelope by a mycobacterial membrane

protein large (MmpL)-type transmembrane protein. This scheme is found for sulfolipid-1, polyacyl trehaloses, and lipooligosaccharides, whose fatty acyl chains are carried by a trehalose core, as well as for phenolic glycolipids and phthiocerol dimycoserates, whose fatty acyl chains are carried by a phthiocerol core ([Daffé et al., 2014](#)). The present work combined with previous data highlight the conservation of this pattern for the mycolate-containing lipids ([Figure 6](#)). However, our data emphasize a fundamental discrepancy with the complex lipids cited above. For the latter, the PKS proteins involved do not contain any TE domain ([Jackson et al., 2007](#)) and the transacylation step is operated by discrete specific polyketide-associated protein (Pap)-type acyltransferases ([Bhatt et al., 2007](#); [Chavadi et al., 2012](#); [Hatzios et al., 2009](#); [Kumar et al., 2007](#); [Onwueme et al., 2004](#); [Rombouts et al., 2011](#)). In contrast, there is no Pap-encoding gene in the vicinity of *pks13* gene on the chromosome ([Cole et al., 1998](#)). Instead, Pks13 is equipped with a TE domain structurally distinct from Pap enzymes, which is responsible for the transfer of the neosynthesized acyl chains onto the trehalose core, as discussed above. This unique mechanism of transfer of PKS products in mycobacteria appears as an extension of the macrocyclisation mechanism, catalyzed by many TE domains, where one nucleophilic atom of the polyketide plays the role of acceptor for the intramolecular transfer of the polyketide carbonyl extremity linked to the catalytic Ser ([Frueh et al., 2008](#)). In the case of TE_{Pks13}, the main difference resides in the fact that the transesterification is intermolecular and not intramolecular, and therefore the domain must adapt an acceptor molecule in its active site, close to the catalytic Ser ([Figure S7](#)). Accordingly, the presence of a hydrophilic pocket that might accommodate trehalose in the TE_{Pks13} domain active site, at an adequate distance for a transacylation reaction, was predicted by molecular modeling. Interestingly, an analogous intermolecular acyltransferase function has been recently reported for the PKS ArmB of the tree pathogen fungus *Armillaria mellea*. ArmB transfers its polyketide products onto a tricyclic sesquiterpene alcohol, generating a cytotoxic melleolide ([Lackner et al., 2013](#)), but the

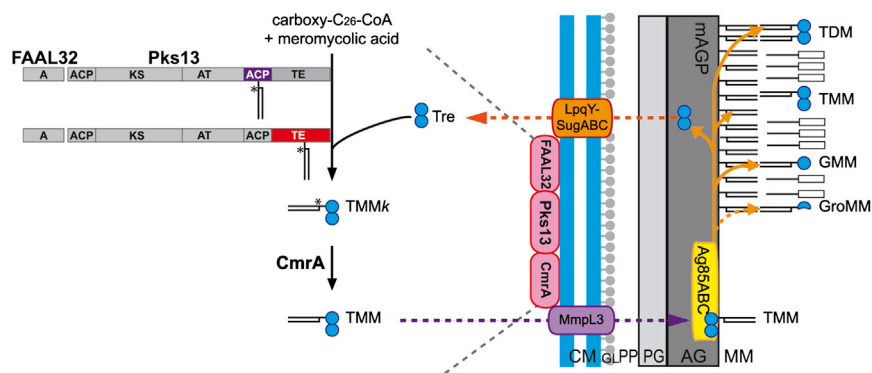


Figure 6. Proposed Schematic of the Last Steps of Mycolic Acid Biosynthesis and Transfer onto the Cell Wall in Mycobacteria

After loading onto Pks13, the acyl chains of carboxy-acyl-CoA and the meromycoloyl-AMP synthesized by FAAL32 are condensed by the enzyme resulting in an α -alkyl β -ketoacyl product linked through a thioester bond to the C-terminal ACP domain. The TE domain of Pks13 cleaves this bond and most likely forms a transient covalent ester bond between the α -alkyl β -ketoacyl chain and the catalytic Ser1533 in its active site. Then, the TE_{Pks13} domain transfers the condensation product onto trehalose to synthesize TMMk. This precursor is then reduced by CmrA into TMM. The latter is exported by MmpL3 membrane trans-

porter, probably into the mycomembrane (MM), where it is used by the mycoloyltransferases (Ag85 complex) tightly associated to the mycomembrane to synthesize biologically active mycolate-containing compounds, i.e., the mAGP complex, the TDM, the GMM, and possibly the GroMM, which constitute major components of the mycomembrane. The released free trehalose is recycled by the LpqY-SugA-SugB-SugC ABC transporter. The scheme is inspired by the present study and previous works quoted in the text. CM, cytoplasmic membrane; GL, granular layer; PP, periplasm; PG, peptidoglycan; AG, arabinogalactan; MM, mycomembrane; *, keto function.

See also Figure S1.

involvement of its TE domain in this step has not been demonstrated yet.

The mycolic acid biosynthesis is the target of the TB drugs isoniazid, ethionamide, and thiacetazone. Furthermore, most of the newly discovered molecules showing promise for the treatment of TB, notably multidrug-resistant TB, inhibit aspects of *M. tuberculosis* cell envelope biogenesis, including the mycolate-containing compound metabolism (Jackson et al., 2013). In particular, target-based screenings focusing on this pathway were successful (North et al., 2014). Given its unique features, the TE_{Pks13} domain constitutes an attractive target for drug development. The recent discovery of a benzofuran molecule both targeting the TE_{Pks13} domain and inhibiting *M. tuberculosis* growth validates this domain as a vulnerable and druggable target (Ioerger et al., 2013). The activity assays with the isolated TE domain and the entire Pks13 enzyme designed during the present work constitute precious tools that we are currently using for the screening of putative anti-TB molecules.

SIGNIFICANCE

The envelope of the tubercle bacillus contains critical pathogenicity factors made of exotic very long chain fatty acids carried by a polyol core. So far, the archetypal building pattern of these complex lipids corresponded to the biosynthesis of the fatty acyl chains by specific polyketide synthases, followed by their transfer onto the polyol moiety catalyzed by a discrete Pap-type acyltransferase. In the specific case of the mycolate-containing compounds, we have previously shown that Pks13 polyketide synthase catalyzes the condensation reaction that produces α -alkyl β -ketoacyl chains, direct precursors of the mycolates (Gavalda et al., 2009). However, the enzymes/domains responsible for the release of the condensation products from Pks13 and for their transfer onto a polyol core remain unknown, leaving gaps in the knowledge of the mycolate-containing compound biosynthesis pathway. In contrast to the current

biosynthesis model suggesting the involvement of a discrete mycoloyl transferase, the present work shows that Pks13 catalyzes itself the cleavage of the thioester bond between the enzyme and the neosynthesized acyl chains. We demonstrate that this function is carried by its thioesterase-like (TE_{Pks13}) domain. Most importantly, the latter exhibits an acyltransferase function and directly transfers the mycolate precursors onto a specific polyol acceptor molecule, trehalose, ultimately leading to the formation of trehalose monomycolate, a common precursor of the mycolate-containing compounds. Thus, the lipid transfer mechanism involved does not use the conventional Pap-type acyltransferases, in conflict with the archetypal biosynthesis pattern of the mycobacterial complex lipids. Whole-cell screening on *M. tuberculosis* has recently shown that the unique TE domain of Pks13 represents a vulnerable and attractive target for drug development to cure tuberculosis (Ioerger et al., 2013).

EXPERIMENTAL PROCEDURES

Protein Production and Purification

See Supplemental Experimental Procedures.

Enzymatic Assays

Condensation assays contained 40 μ M [14 C]₁₄ acid (specific activity: 54 mCi/mmol, American Radiolabeled Chemicals) and 40 μ M carboxy-C₁₆-CoA (synthesized and purified as described previously [Gavalda et al., 2009]), 8 mM MgCl₂, and 2 mM ATP, in 50 mM HEPES (pH 7.2). The reactions (total volume: 10 μ l) were started by the addition of 1–2 μ M FAAL32 and 2 μ M Pks13, incubated for 6 hr at 30°C, then stopped at –20°C. Control experiments without certain reagents or using heat-inactivated Pks13 (heated 10 min at 95°C) were performed, as mentioned in the text or figure legends. For MS analyses, condensation assays were run in the same conditions with cold substrates, in 100 μ l final volume. The effect of putative acceptor molecules was evaluated by adding them at various concentrations, as mentioned in the text or figure legends, in the presence of enzymes from glycerol-free stocks. In vitro complementation assays were performed in the presence of 200 mM trehalose and 500 mM glycerol, 1 μ M FAAL32, and 1 μ M of either WT Pks13 or Pks13 S1533A, \pm 4 or 8 μ M of purified TE_{Pks13} domain. The reaction media were either kept intact or submitted to the following treatment: samples were mixed with

100 μ l tetrahydrofuran and reduced for 1 hr by adding 500 μ l NaBH₄ 0.5 M in ethanol 99%; reactions were stopped by addition of 1 ml acetic acid; for saponification, 1.5 ml KOH 10% (w/v) in CH₃OH:toluene, 8:2 were added and samples incubated for 1 hr at 80°C; the media were then acidified with 2 ml H₂SO₄; and lipids were extracted with diethylether, washed with water, dried, and methylated with diazomethane (Figure 5C). Thioesterase and acyltransferase activity assays were performed with either 40 μ M [¹⁻¹⁴C]C₁₆-CoA (specific activity: 60 mCi/mmol, Perkin Elmer) or cold C₁₆-CoA (for MS analysis), 100 mM (for TE_{Pks13} assays) or variable concentrations (for Pks13; specified in Figure 4) of putative acceptor, and either 2 μ M Pks13 or 4 μ M TE_{Pks13} domain, in 50 mM HEPES (pH 7.2), incubated for 6 hr at 30°C, then frozen at -20°C. For all assays, the solvent coming from the substrate solutions was evaporated before addition of the other reagents. All assays were performed at least in three independent experiments. K_m were measured in the presence of TE_{Pks13} (2 μ M), a fixed concentration of [¹⁻¹⁴C]C₁₆-CoA (40 μ M), and variable concentrations of trehalose (0.01–200 mM) or glucose (0.5–1000 mM; higher concentrations could not be used because of problems of solubility and migration on thin layer). The experimental conditions were selected in order to be in a linear response range. Data were fitted to the Michaelis-Menten equation by least-squares fits to a hyperbola using the program GraphPad Prism version 5.04.

TLC Analyses

See also [Supplemental Experimental Procedures](#). Intact media of condensation assays and thioesterase/transacylase activity assays were analyzed by TLC on silica gel G60 plates developed with CHCl₃/CH₃OH/H₂O 65/25/4 and butan-1-ol/acetic acid/water 80/25/40, respectively. The lipid extracts from reaction media or purified compounds submitted to chemical treatment were spotted on TLC plates as diethylether solutions and developed with dichloromethane. The radiolabeling was detected by phosphorimaging (Variable Mode Imager Typhoon TRIO, Amersham Biosciences) and quantified in arbitrary units using the ImageQuant version 5.1 software (Molecular Dynamics).

MALDI-TOF MS and MS/MS

See [Supplemental Experimental Procedures](#).

Homology Modeling, Structural Comparison, and Visualization

See details in [Supplemental Experimental Procedures](#). The SWISS-MODEL program (www.swissmodel.expasy.org) (Arnold et al., 2006) was used to generate a homology model from the sequence of the TE_{Pks13} domain. Structure visualization and analyses were carried out using the PyMOL program (www.pymol.org).

SUPPLEMENTAL INFORMATION

Supplemental Information includes Supplemental Experimental Procedures, seven figures, and one table and can be found with this article online at <http://dx.doi.org/10.1016/j.chembiol.2014.10.011>.

AUTHOR CONTRIBUTIONS

S.G., F.B., L.M., and A.Q. conceived and designed experiments; S.G., F.B., F.L., L.M., and A.Q. performed research; S.G. and F.B. performed radiolabeled activity assays, competition experiments, and TLC/phosphorimaging analyses; S.G. made all chemical treatments of reaction products; F.B. performed cold activity assays for MALDI-TOF MS analysis and TE_{Pks13} kinetic experiments; F.L., C.B., W.M., C.C., and C.G. contributed to reagents, material, or analysis tools; S.G., F.B., F.L., L.M., M.D., and A.Q. analyzed data; M.D. and A.Q. supervised the project; S.G., L.M., and A.Q. created the figures; and A.Q. wrote the paper. Most authors commented or contributed to sections of the manuscript.

ACKNOWLEDGMENTS

We are grateful to Dr. Anne Lemassu and Lucie Spina for performing some analytical assays, to Dr. Henri Montrozier for synthesizing carboxyacyl-CoA, to Dr. Hedia Marrakchi for the generous gift of purified FAAL32, and to Dr. Marie-Antoinette Lan  elle and Prof. Marielle Tropis for fruitful discussions. This work was supported by the "Vaincre la Mucoviscidose" (IC0716, France),

the European Community (TB-drug, grant LSHP-CT-2006-037217), the Agence Nationale de la Recherche (XPKS-MYCO, grant 09-BLAN-0298-01 and FASMY, grant ANR-14-CE16-0012), and the R  gion Midi-Pyr  n  es (MYCA, FEDER grant 34249).

Received: July 15, 2014
Revised: October 10, 2014
Accepted: October 15, 2014
Published: November 26, 2014

REFERENCES

- Anderson, D.H., Harth, G., Horwitz, M.A., and Eisenberg, D. (2001). An interfacial mechanism and a class of inhibitors inferred from two crystal structures of the *Mycobacterium tuberculosis* 30 kDa major secretory protein (Antigen 85B), a mycolyl transferase. *J. Mol. Biol.* 307, 671–681.
- Arnold, K., Bordoli, L., Kopp, J., and Schwede, T. (2006). The SWISS-MODEL workspace: a web-based environment for protein structure homology modeling. *Bioinformatics* 22, 195–201.
- Belisle, J.T., Vissa, V.D., Sievert, T., Takayama, K., Brennan, P.J., and Besra, G.S. (1997). Role of the major antigen of *Mycobacterium tuberculosis* in cell wall biogenesis. *Science* 276, 1420–1422.
- Besra, G.S., Sievert, T., Lee, R.E., Slayden, R.A., Brennan, P.J., and Takayama, K. (1994). Identification of the apparent carrier in mycolic acid synthesis. *Proc. Natl. Acad. Sci. USA* 91, 12735–12739.
- Bhatt, K., Gurucha, S.S., Bhatt, A., Besra, G.S., and Jacobs, W.R., Jr. (2007). Two polyketide-synthase-associated acyltransferases are required for sulfolipid biosynthesis in *Mycobacterium tuberculosis*. *Microbiology* 153, 513–520.
- Bhatt, A., Brown, A.K., Singh, A., Minnikin, D.E., and Besra, G.S. (2008). Loss of a mycobacterial gene encoding a reductase leads to an altered cell wall containing beta-oxo-mycolic acid analogs and accumulation of ketones. *Chem. Biol.* 15, 930–939.
- Bou Raad, R., M  n  che, X., de Sousa-d'Auria, C., Chami, M., Salmeron, C., Tropis, M., Labarre, C., Daff  , M., Houssin, C., and Bayan, N. (2010). A deficiency in arabinogalactan biosynthesis affects *Corynebacterium glutamicum* mycolate outer membrane stability. *J. Bacteriol.* 192, 2691–2700.
- Chavadi, S.S., Onwueme, K.C., Edupuganti, U.R., Jerome, J., Chatterjee, D., Soll, C.E., and Quadri, L.E. (2012). The mycobacterial acyltransferase PapA5 is required for biosynthesis of cell wall-associated phenolic glycolipids. *Microbiology* 158, 1379–1387.
- Cole, S.T., Brosch, R., Parkhill, J., Garnier, T., Churcher, C., Harris, D., Gordon, S.V., Eiglmeier, K., Gas, S., Barry, C.E., 3rd., et al. (1998). Deciphering the biology of *Mycobacterium tuberculosis* from the complete genome sequence. *Nature* 393, 537–544.
- Daff  , M., Crick, D.C., and Jackson, M. (2014). Genetics of capsular polysaccharides and cell envelope (glyco)lipids. In *Molecular Genetics of Mycobacteria*, G.F. Hatfull and W.R. Jacobs, Jr., eds. (Washington, DC: ASM Press), pp. 559–609.
- Datta, A.K., and Takayama, K. (1993). Biosynthesis of a novel 3-oxo-2-tetradecyloctadecanoate-containing phospholipid by a cell-free extract of *Corynebacterium diphtheriae*. *Biochim. Biophys. Acta* 1169, 135–145.
- Esin, S., Counoupas, C., Alicino, A., Brancatisano, F.L., Maisetta, G., Bottai, D., Di Luca, M., Florio, W., Campa, M., and Batoni, G. (2013). Interaction of *Mycobacterium tuberculosis* cell wall components with the human natural killer cell receptors Nkp44 and Toll-like receptor 2. *Scand. J. Immunol.* 77, 460–469.
- Frueh, D.P., Arthanari, H., Koglin, A., Vosburg, D.A., Bennett, A.E., Walsh, C.T., and Wagner, G. (2008). Dynamic thiolation-thioesterase structure of a non-ribosomal peptide synthetase. *Nature* 454, 903–906.
- Gavalda, S., L  ger, M., van der Rest, B., Stella, A., Bardou, F., Montrozier, H., Chalut, C., Buret-Schiltz, O., Marrakchi, H., Daff  , M., and Qu  mard, A. (2009). The Pks13/FadD32 crosstalk for the biosynthesis of mycolic acids in *Mycobacterium tuberculosis*. *J. Biol. Chem.* 284, 19255–19264.
- Gebhardt, H., Meniche, X., Tropis, M., Kr  mer, R., Daff  , M., and Morbach, S. (2007). The key role of the mycolic acid content in the functionality of the cell wall permeability barrier in *Corynebacterineae*. *Microbiology* 153, 1424–1434.

- Geisel, R.E., Sakamoto, K., Russell, D.G., and Rhoades, E.R. (2005). In vivo activity of released cell wall lipids of *Mycobacterium bovis* bacillus Calmette-Guérin is due principally to trehalose mycolates. *J. Immunol.* **174**, 5007–5015.
- Glickman, M.S. (2008). Cording, cord factors, and trehalose dimycolate. In *The Mycobacterial Cell Envelope*, M. Daffé and J.M. Reyraat, eds. (Washington, DC: ASM Press), pp. 63–73.
- Grzegorzewicz, A.E., Pham, H., Gundi, V.A., Scherman, M.S., North, E.J., Hess, T., Jones, V., Gruppo, V., Born, S.E., Korduláková, J., et al. (2012). Inhibition of mycolic acid transport across the *Mycobacterium tuberculosis* plasma membrane. *Nat. Chem. Biol.* **8**, 334–341.
- Hatzios, S.K., Schelle, M.W., Holsclaw, C.M., Behrens, C.R., Botyanszki, Z., Lin, F.L., Carlson, B.L., Kumar, P., Leary, J.A., and Bertozzi, C.R. (2009). PapA3 is an acyltransferase required for polyacyltrehalose biosynthesis in *Mycobacterium tuberculosis*. *J. Biol. Chem.* **284**, 12745–12751.
- Hertweck, C. (2009). The biosynthetic logic of polyketide diversity. *Angew. Chem. Int. Ed. Engl.* **48**, 4688–4716.
- Ioerger, T.R., O'Malley, T., Liao, R., Guinn, K.M., Hickey, M.J., Mohaideen, N., Murphy, K.C., Boshoff, H.I., Mizrahi, V., Rubin, E.J., et al. (2013). Identification of new drug targets and resistance mechanisms in *Mycobacterium tuberculosis*. *PLoS ONE* **8**, e75245.
- Jackson, M., Raynaud, C., Lanéeelle, M.A., Guilhot, C., Laurent-Winter, C., Ensergueix, D., Gicquel, B., and Daffé, M. (1999). Inactivation of the antigen 85C gene profoundly affects the mycolate content and alters the permeability of the *Mycobacterium tuberculosis* cell envelope. *Mol. Microbiol.* **31**, 1573–1587.
- Jackson, M., Stadthagen, G., and Gicquel, B. (2007). Long-chain multiple methyl-branched fatty acid-containing lipids of *Mycobacterium tuberculosis*: biosynthesis, transport, regulation and biological activities. *Tuberculosis (Edinb.)* **87**, 78–86.
- Jackson, M., McNeil, M.R., and Brennan, P.J. (2013). Progress in targeting cell envelope biogenesis in *Mycobacterium tuberculosis*. *Future Microbiol.* **8**, 855–875.
- Kalscheuer, R., Weinrick, B., Veeraraghavan, U., Besra, G.S., and Jacobs, W.R., Jr. (2010). Trehalose-recycling ABC transporter LpqY-SugA-SugB-SugC is essential for virulence of *Mycobacterium tuberculosis*. *Proc. Natl. Acad. Sci. USA* **107**, 21761–21766.
- Kizawa, H., Miyagawa, K., and Sugiyama, Y. (1995). Purification and characterization of trehalose phosphorylase from *Micrococcus varians*. *Biosci. Biotechnol. Biochem.* **59**, 1908–1912.
- Koglin, A., and Walsh, C.T. (2009). Structural insights into nonribosomal peptide enzymatic assembly lines. *Nat. Prod. Rep.* **26**, 987–1000.
- Kumar, P., Schelle, M.W., Jain, M., Lin, F.L., Petzold, C.J., Leavell, M.D., Leary, J.A., Cox, J.S., and Bertozzi, C.R. (2007). PapA1 and PapA2 are acyltransferases essential for the biosynthesis of the *Mycobacterium tuberculosis* virulence factor sulfolipid-1. *Proc. Natl. Acad. Sci. USA* **104**, 11221–11226.
- Lackner, G., Bohnert, M., Wick, J., and Hoffmeister, D. (2013). Assembly of melleotide antibiotics involves a polyketide synthase with cross-coupling activity. *Chem. Biol.* **20**, 1101–1106.
- Layre, E., Collmann, A., Bastian, M., Mariotti, S., Czaplicki, J., Prandi, J., Mori, L., Stenger, S., De Libero, G., Puzo, G., and Gilleron, M. (2009). Mycolic acids constitute a scaffold for mycobacterial lipid antigens stimulating CD1-restricted T cells. *Chem. Biol.* **16**, 82–92.
- Lea-Smith, D.J., Pyke, J.S., Tull, D., McConville, M.J., Coppel, R.L., and Crellin, P.K. (2007). The reductase that catalyzes mycolic motif synthesis is required for efficient attachment of mycolic acids to arabinogalactan. *J. Biol. Chem.* **282**, 11000–11008.
- Léger, M., Gavalda, S., Guillet, V., van der Rest, B., Slama, N., Montrozier, H., Mourey, L., Quémard, A., Daffé, M., and Marrakchi, H. (2009). The dual function of the *Mycobacterium tuberculosis* FadD32 required for mycolic acid biosynthesis. *Chem. Biol.* **16**, 510–519.
- Marchand, C.H., Salmeron, C., Bou Raad, R., Méniche, X., Chami, M., Masi, M., Blanot, D., Daffé, M., Tropis, M., Huc, E., et al. (2012). Biochemical disclosure of the mycolate outer membrane of *Corynebacterium glutamicum*. *J. Bacteriol.* **194**, 587–597.
- Marrakchi, H., Lanéeelle, M.A., and Daffé, M. (2014). Mycolic acids: structures, biosynthesis, and beyond. *Chem. Biol.* **21**, 67–85.
- Moody, D.B., Briken, V., Cheng, T.Y., Roura-Mir, C., Guy, M.R., Geho, D.H., Tykocinski, M.L., Besra, G.S., and Porcelli, S.A. (2002). Lipid length controls antigen entry into endosomal and nonendosomal pathways for CD1b presentation. *Nat. Immunol.* **3**, 435–442.
- North, E.J., Jackson, M., and Lee, R.E. (2014). New approaches to target the mycolic acid biosynthesis pathway for the development of tuberculosis therapeutics. *Curr. Pharm. Des.* **20**, 4357–4378.
- Onwueme, K.C., Ferreras, J.A., Buglino, J., Lima, C.D., and Quadri, L.E. (2004). Mycobacterial polyketide-associated proteins are acyltransferases: proof of principle with *Mycobacterium tuberculosis* PapA5. *Proc. Natl. Acad. Sci. USA* **101**, 4608–4613.
- Portevin, D., De Sousa-D'Auria, C., Houssin, C., Grimaldi, C., Chami, M., Daffé, M., and Guilhot, C. (2004). A polyketide synthase catalyzes the last condensation step of mycolic acid biosynthesis in mycobacteria and related organisms. *Proc. Natl. Acad. Sci. USA* **101**, 314–319.
- Promé, J.C., Walker, R.W., and Lacave, C. (1974). Condensation de deux molécules d'acide palmitique chez *Corynebacterium diphtheriae*: formation d'un béta-céto-ester de tréhalose. *C. R. Acad. Sci.* **278**, 1065–1068.
- Puzo, G., Tissie, G., Aurelle, H., Lacave, C., and Promé, J.C. (1979). Occurrence of 3-oxo-acyl groups in the 6,6'-diesters of alpha-D-trehalose. New glycolipids related to cord factor from *Corynebacterium diphtheriae*. *Eur. J. Biochem.* **98**, 99–105.
- Riby, J., and Galand, G. (1985). Rat intestinal brush border membrane trehalase: some properties of the purified enzyme. *Comp. Biochem. Physiol. B* **82**, 821–827.
- Rombouts, Y., Alibaud, L., Carrère-Kremer, S., Maes, E., Tokarski, C., Ellass, E., Kremer, L., and Guérardel, Y. (2011). Fatty acyl chains of *Mycobacterium marinum* lipooligosaccharides: structure, localization and acylation by PapA4 (MMAR_2343) protein. *J. Biol. Chem.* **286**, 33678–33688.
- Shimakata, T., Tsubokura, K., and Kusaka, T. (1986). Requirement of glucose for mycolic acid biosynthetic activity localized in the cell wall of *Bacterionema matruchotii*. *Arch. Biochem. Biophys.* **247**, 302–311.
- Tahlan, K., Wilson, R., Kastrinsky, D.B., Arora, K., Nair, V., Fischer, E., Barnes, S.W., Walker, J.R., Alland, D., Barry, C.E., 3rd, and Boshoff, H.I. (2012). SQ109 targets MmpL3, a membrane transporter of trehalose monomycolate involved in mycolic acid donation to the cell wall core of *Mycobacterium tuberculosis*. *Antimicrob. Agents Chemother.* **56**, 1797–1809.
- Takayama, K., Wang, C., and Besra, G.S. (2005). Pathway to synthesis and processing of mycolic acids in *Mycobacterium tuberculosis*. *Clin. Microbiol. Rev.* **18**, 81–101.
- Tropis, M., Meniche, X., Wolf, A., Gebhardt, H., Strelkov, S., Chami, M., Schomburg, D., Krämer, R., Morbach, S., and Daffé, M. (2005). The crucial role of trehalose and structurally related oligosaccharides in the biosynthesis and transfer of mycolic acids in *Corynebacterineae*. *J. Biol. Chem.* **280**, 26573–26585.
- Varela, C., Rittmann, D., Singh, A., Krumbach, K., Bhatt, K., Eggeling, L., Besra, G.S., and Bhatt, A. (2012). MmpL genes are associated with mycolic acid metabolism in mycobacteria and corynebacteria. *Chem. Biol.* **19**, 498–506.
- Vilchêze, C., Morbidoni, H.R., Weisbrod, T.R., Iwamoto, H., Kuo, M., Sacchetti, J.C., and Jacobs, W.R., Jr. (2000). Inactivation of the inhA-encoded fatty acid synthase II (FASII) enoyl-acyl carrier protein reductase induces accumulation of the FASII end products and cell lysis of *Mycobacterium smegmatis*. *J. Bacteriol.* **182**, 4059–4067.
- Walsh, C.T., Gehring, A.M., Weinreb, P.H., Quadri, L.E., and Flugel, R.S. (1997). Post-translational modification of polyketide and nonribosomal peptide synthases. *Curr. Opin. Chem. Biol.* **1**, 309–315.
- WHO (2013). *Global tuberculosis report 2013*. (Geneva: WHO Press).
- Zhang, W., Chakravarty, B., Zheng, F., Gu, Z., Wu, H., Mao, J., Wakil, S.J., and Quiocho, F.A. (2011). Crystal structure of FAS thioesterase domain with polyunsaturated fatty acyl adduct and inhibition by dihomogamma-linolenic acid. *Proc. Natl. Acad. Sci. USA* **108**, 15757–15762.

Chemistry & Biology, Volume 21

Supplemental Information

The Polyketide Synthase Pks13 Catalyzes

a Novel Mechanism of Lipid Transfer

in Mycobacteria

Sabine Gavaldà, Fabienne Bardou, Françoise Laval, Cécile Bon, Wladimir Malaga, Christian Chalut, Christophe Guilhot, Lionel Mourey, Mamadou Daffé, and Annaïk Quémard

INVENTORY OF SUPPLEMENTAL INFORMATION

Supplemental Data

Figure S1 (related to Introduction and Figure 6). Schematic of the mycolic condensation reaction

Figure S2 (related to Figure 1). MALDI-TOF/TOF MS/MS analysis of Pks13 condensation products

Figure S3 (related to Figure 1). Analysis of the purified Pks13 product *e*

Figure S4 (related to Figure 1). Influence of acceptor concentration on the nature of Pks13 products

Figure S5 (related to Figure 3). Prediction of a fatty acyl binding tunnel in TE_{Pks13} model

Figure S6 (related to Figure 4). SDS-PAGE analysis of FPLC purification steps of recombinant TE_{Pks13} domain

Figure S7 (related to Figure 5). Schematic representation of the reaction mechanism catalyzed by TE_{Pks13} domain

Table S1 (related to Figure 4). MALDI-TOF MS analysis of the reactions catalyzed by TE_{Pks13} domain in the presence of C₁₆-CoA and different types of acceptor

Supplemental Experimental Procedures

Supplemental References

SUPPLEMENTAL DATA

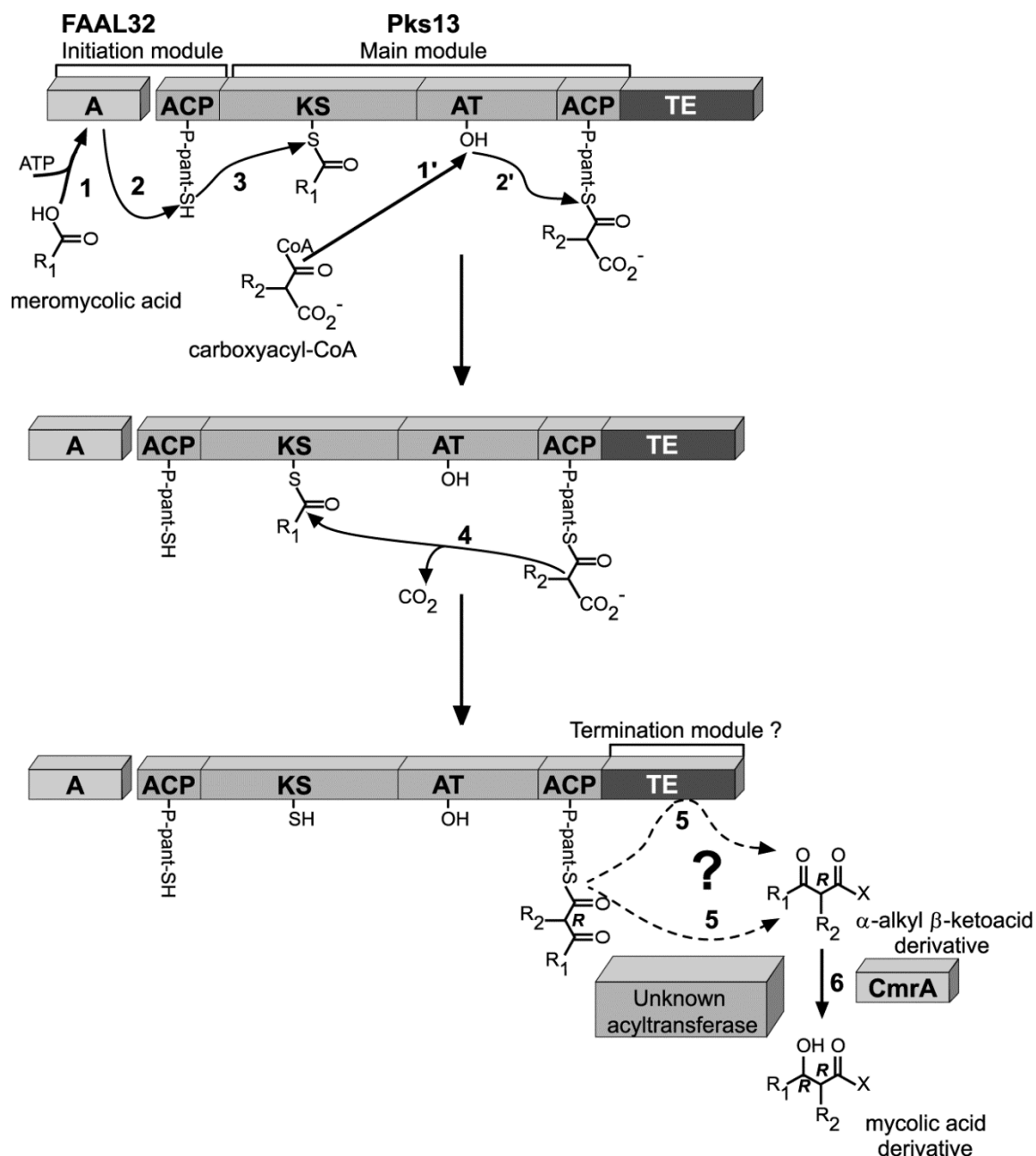


Figure S1 (related to Introduction). Schematic of the mycolic condensation reaction

The meromycoloyl chain is loaded by FAAL32 adenylation enzyme (A) onto the N-terminal ACP domain of Pks13 [1-2], then transferred onto the ketosynthase (KS) domain [3]; the acyltransferase domain (AT) loads the carboxylated fatty acyl chain onto the C-terminal ACP domain [1'-2']; the KS domain catalyzes a Claisen-type condensation between both acyl chains [4], leading to the synthesis of a α -alkyl β -ketoacyl product bound to the P-pant arm of the C-terminal ACP domain. The mechanism of release of the condensation products from Pks13 remains unknown; it might involve the C-terminal putative thioesterase domain of Pks13 (TE_{Pks13}) or a discrete unknown acyltransferase [5]. The reduction of the β -keto function into a secondary alcohol function is catalyzed by CmrA [6]. In mycobacteria, $R_1 = C_{41}$ - C_{61} , $R_2 = C_{20}$ - C_{24} ; in corynebacteria, $R_1 = C_7$ - C_{17} , $R_2 = C_6$ - C_{16} . X = putative unknown moiety or -OH.

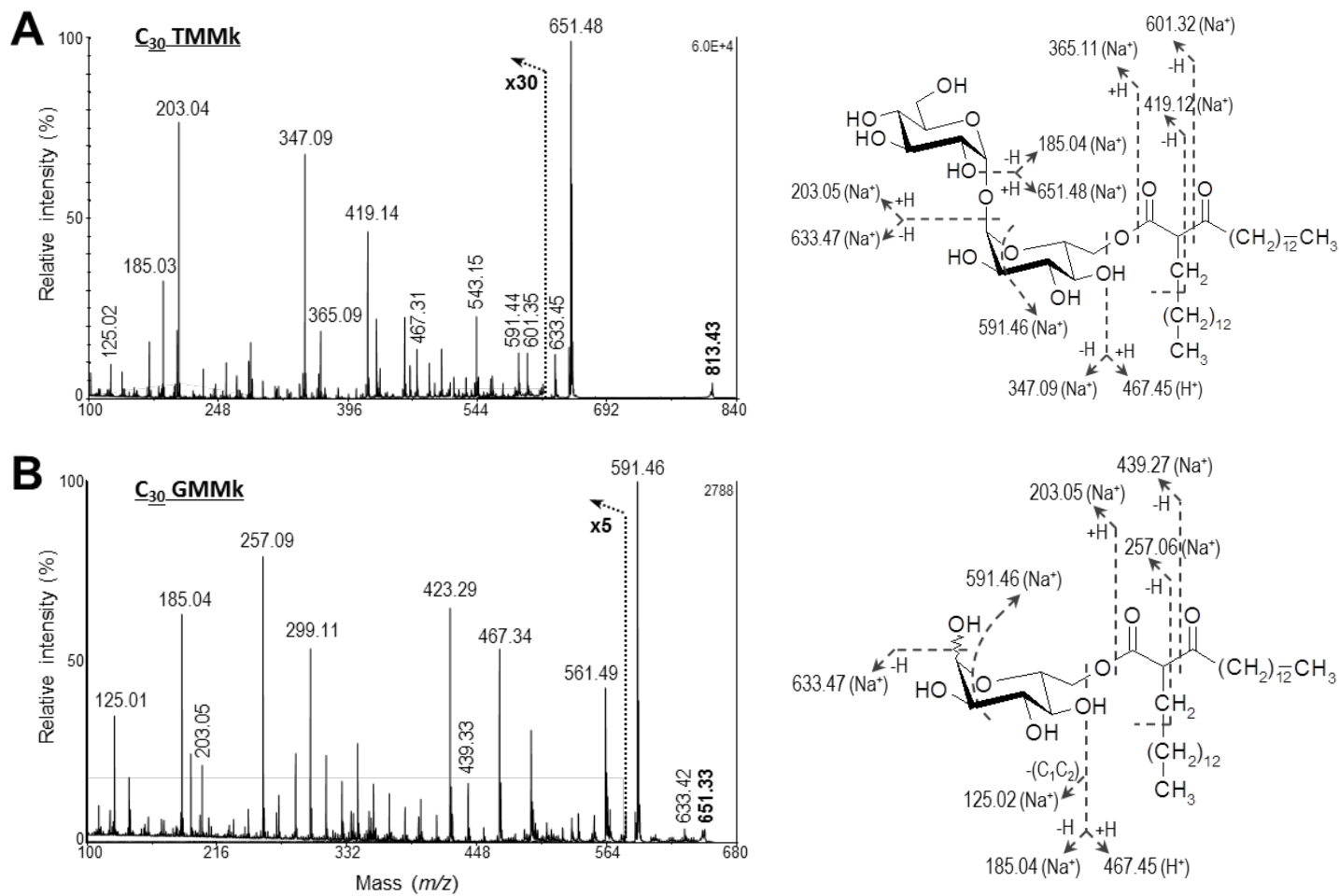


Figure S2 (related to Figure 1). MALDI-TOF/TOF MS/MS analysis of Pks13 condensation products

The precursor ions are labelled in bold in the spectra. The main identified fragment ions (with their theoretical *m/z* values) are indicated in the fragmentation schematics.

(A) MS/MS spectrum of the C₃₀ TMMk. Identical fragmentations were detected for the C₃₂ TMMk (data not shown).

(B) MS/MS spectrum of the C₃₀ GMMk. Identical fragmentations were detected for the C₃₂ GMMk (data not shown).

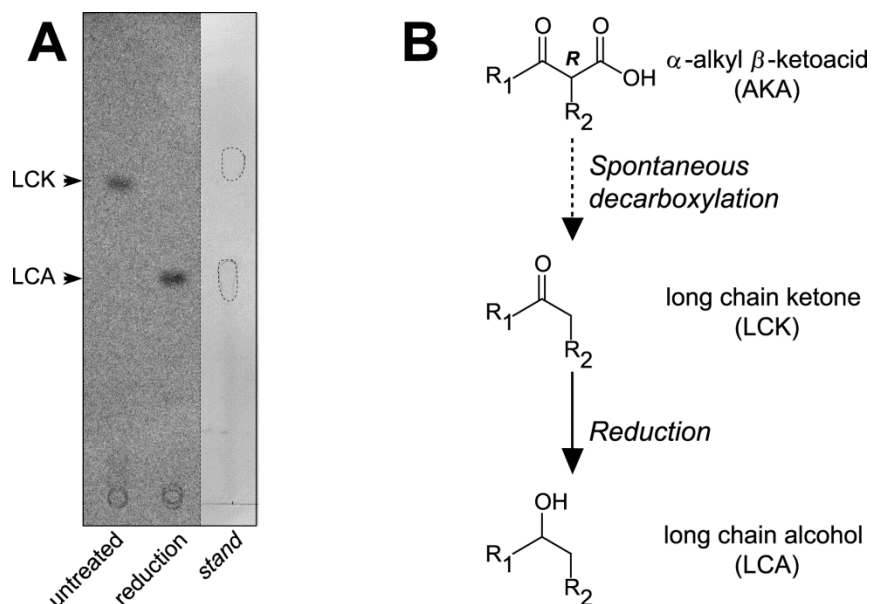


Figure S3 (related to Figure 1). Analysis of the purified Pks13 product *e*

(A) Silica gel TLC/phosphorimaging. Product *e* was spotted either in a native form (*untreated*) or after reduction by $NaBH_4$ (*reduction*). *Stand*, C_{31} long chain ketone (LCK) and long chain alcohol (LCA) standards revealed under UV light after rhodamine spraying. Eluent: CH_2Cl_2 .

(B) Fate of α -alkyl β -ketoacids released by FAAL32-Pks13. The labile α -alkyl β -ketoacids are spontaneously decarboxylated into long chain ketones (Ahibo-Coffy et al., 1978), which give long chain alcohols after chemical reduction.

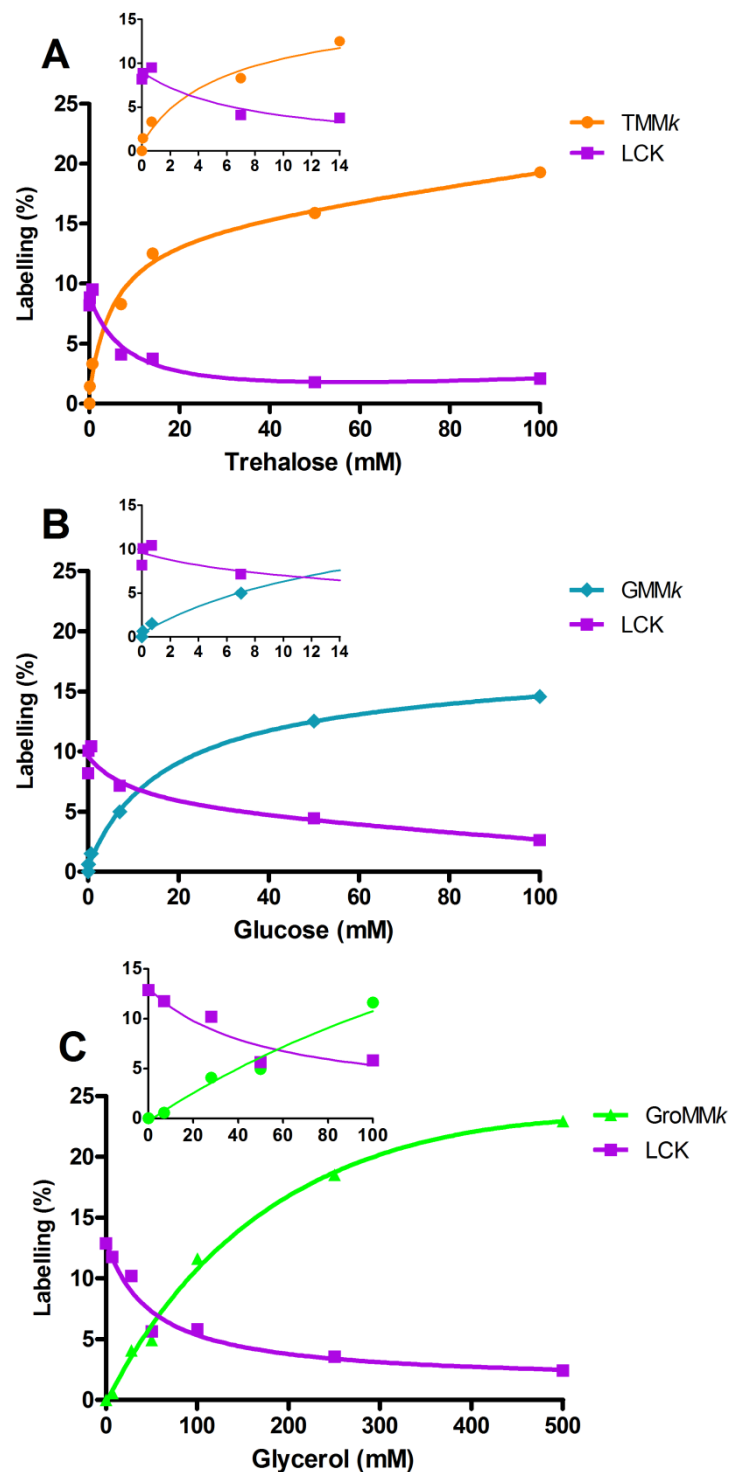


Figure S4 (related to Figure 1). Influence of acceptor concentration on the nature of Pks13 products

The biosynthesis yield of each α -alkyl β -ketoacyl derivative was measured by TLC/phosphorimaging analysis of untreated reaction media for assays in the presence of a concentration range of a single acceptor molecule: (A) trehalose, (B) glucose or (C) glycerol. Data are expressed as percentages of labeling with respect to the total TLC lane labeling.

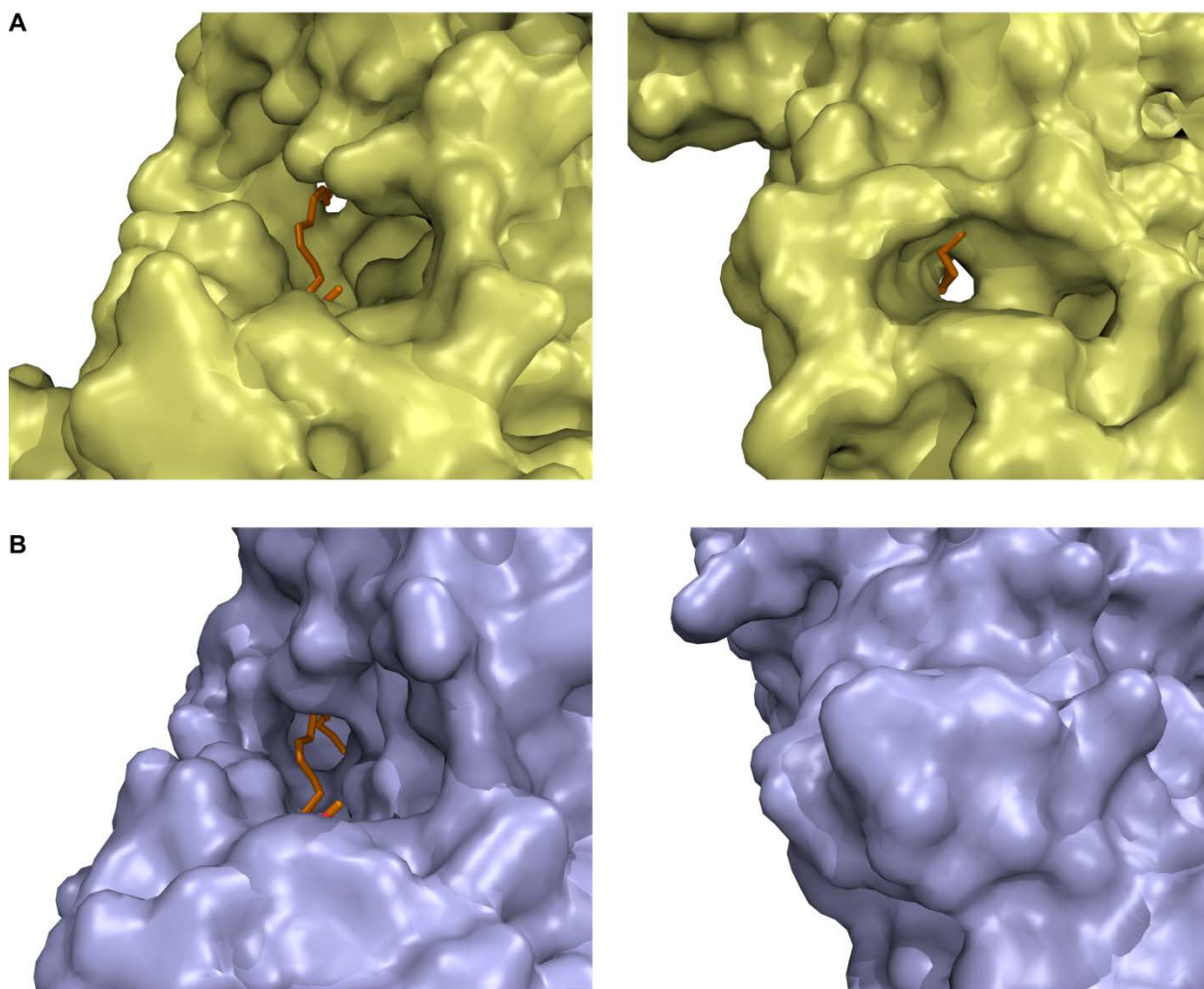


Figure S5 (related to Figure 3). Visualization of a fatty acyl-binding groove-tunnel in TE_{Pks13} model.

(A) Surface representation of the predicted fatty acyl-binding groove-tunnel in TE_{Pks13} domain. A rotation of +165° according to the x axis links the left and right panels.

(B) Surface representation of the fatty acyl-binding groove-tunnel in TE_{hFAS} domain (PDB-3TJM) (Zhang et al., 2011). Orientations are as in (A). The polyunsaturated ligand, methyl γ -linolenylfluorophosphonate, bound to TE_{hFAS} domain is drawn as orange sticks.

As shown in the right panels, the end of the tunnel is closed in TE_{hFAS} domain; the groove-tunnel has the adequate length to fit a regular-size (C₁₆-C₁₈) fatty acyl chain (Zhang et al., 2011). In contrast, the predicted groove-tunnel in TE_{Pks13} is open and communicates with other grooves and tunnels, which might accommodate the very long α -alkyl β -ketoacyl chain produced by Pks13.

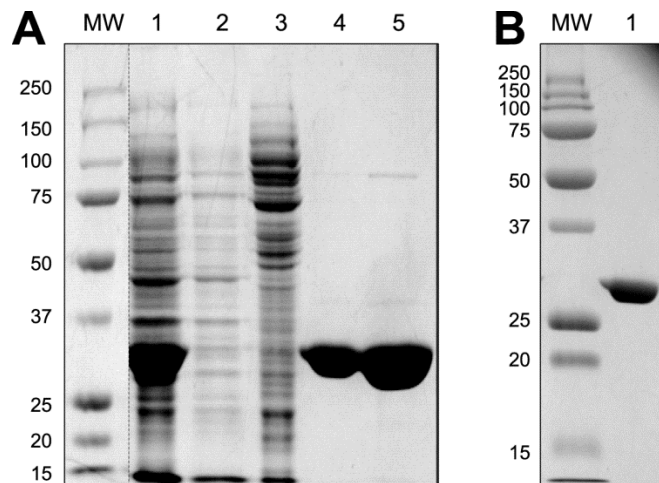


Figure S6 (related to Figure 4). SDS-PAGE analysis of FPLC purification steps of recombinant TE_{Pks13} domain

Coomassie blue staining. MW, molecular weight markers.

(A) Ni Chelating Fast Flow column. 12% polyacrylamide gel. Lane 1, total soluble proteins; lane 2, flow through; lane 3, contaminating protein fraction; lanes 4-5, His₆-tagged TE_{Pks13}-containing fractions.

(B) HiLoad 16/60 Superdex 75 column. 15% polyacrylamide gel. Lane 1, pool of untagged TE_{Pks13}-containing fractions.

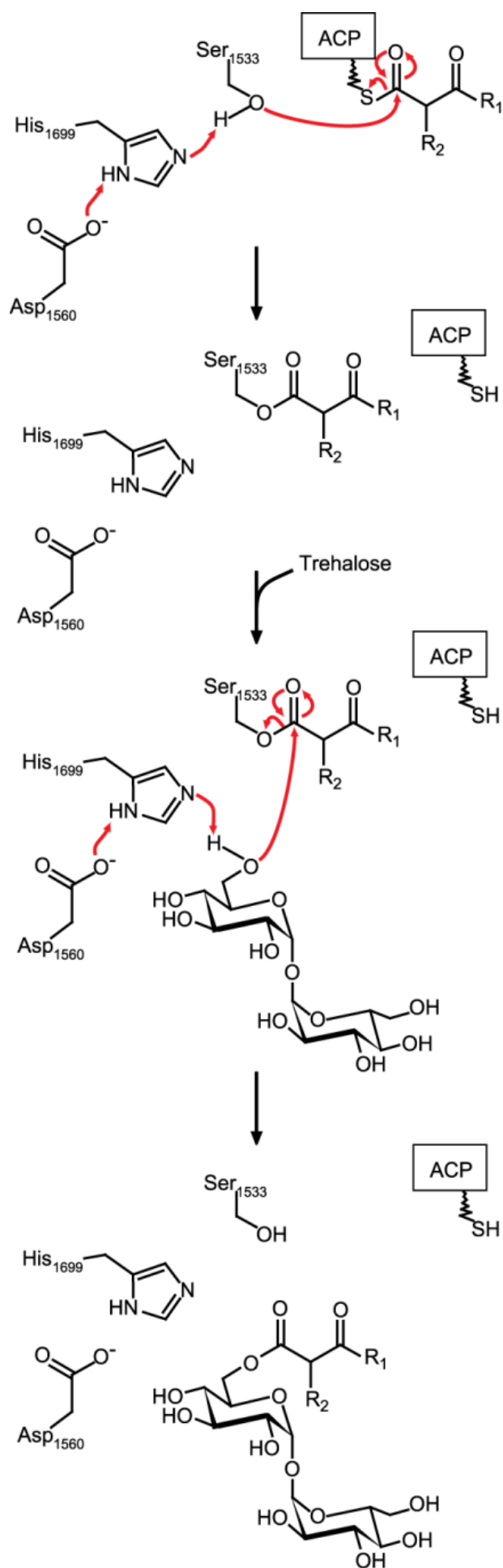


Figure S7 (related to Figure 5). Schematic representation of the reaction mechanism catalyzed by TE_{Pks13} domain

The thioester bond between the neosynthesized α -alkyl β -ketoacyl chain and the P-pant arm carried by Pks13 C-terminal ACP domain is cleaved and the product is transferred onto the catalytic Ser₁₅₃₃ residue. The acyl chain is then loaded *via* an intermolecular transacylation reaction onto the 6-hydroxy group of the trehalose acceptor, activated by the catalytic His₁₆₉₉. In TE domains that catalyze a hydrolysis, the His residue activates a water molecule, whereas in TE domains catalyzing a macrocyclization, the ester bond of the polyketide-enzyme intermediate is submitted to an intramolecular nucleophilic attack, e.g. by a polyketide secondary alcohol function activated by the catalytic His.

Table S1 (related to Figure 4). MALDI-TOF MS analysis of the reactions catalyzed by TE_{Pks13} domain in the presence of C₁₆-CoA and different types of acceptor

Putative acceptor molecule/treatment	Acyl chain(s)	Calculated mass of monosodium adduct ^a	Detected experimental mass (<i>m/z</i>)	Compound	Abbreviation	Label
trehalose	1 x C ₁₆	603.34	603.34 ^b	monopalmitoyl trehalose	C16-Tre	α
	2 x C ₁₆	841.56	841.56 ^b	dipalmitoyl trehalose	diC16-Tre	β
glucose	1 x C ₁₆	441.28	441.27 ^b	monopalmitoyl glucose	C16-Glc	χ
glycerol	1 x C ₁₆	353.27	353.25 ^b	monopalmitoyl glycerol	C16-Gro	δ
	2 x C ₁₆	591.50	591.48 ^b	dipalmitoyl glycerol	diC16-Gro	δ'
maltose	1 x C ₁₆	603.34	603.32 ^b	monopalmitoyl maltose	C16-Mal	α'
none	C ₁₆	279.23	279.15	C ₁₆ acid	C ₁₆	–

^amass calculated by Data Explorer software (Applied Biosystems). ^bion peaks exclusively detected in the corresponding sample.

SUPPLEMENTAL EXPERIMENTAL PROCEDURES

Protein production and purification

The phosphopantetheinylated Pks13 protein was produced in *Escherichia coli* by coexpressing the *pks13* (*Rv3800c*) gene of *M. tuberculosis* H37Rv with the *sfp* gene encoding the P-pant transferase from *Bacillus subtilis* and purified as described previously (Gavalda et al., 2009). The vector used for the production of the Pks13 S1533A mutant isoenzyme was constructed by double-strand site-directed mutagenesis with the inverse-PCR technique (Weiner et al., 1994) using the WT *pks13* expressing vector and oligonucleotides 5'-CTAGGCGGTGTGCTGGCCTACG-3' and 5'-GGCCCAACCCACCAGGACATAGG-3'. The resulting construct was checked by DNA sequencing. Recombinant FAAL32 (*Rv3801c*) protein of *M. tuberculosis* H37Rv was produced and purified as described previously (Leger et al., 2009). The DNA encoding TE_{Pks13} domain (positions 4309-5175 bp) was amplified by PCR from *M. tuberculosis* H37Rv genomic DNA using primers 5'-TTCATATGGAGGCGCTGGCCGACAAG-3' and 5'-TTAAGCTTATCGGCCTCGATCTGCCC-3' and cloned between the NdeI and HindIII sites of pET28aII, a derivative of the pET28a expression vector (Novagen), to yield pWM69. The pET28aII vector was constructed by inserting a DNA linker harboring a stop codon, which was prepared by annealing primers 5'-AGCTTTGACAGGTACCATC-3' and 5'-TCGAGATGGTACCTGTCAA-3' between the XhoI and HindIII sites of pET-28a. pWM69 was then transferred in the *E. coli* BL21 (DE3) pLysS strain (Novagen) and the resulting strain was grown at 37 °C in terrific broth medium (Invitrogen) supplemented with chloramphenicol (25 µg/ml) and kanamycin (35 µg/ml) until an OD_{600nm} of 0.6-0.9. It was then induced with 1 mM IPTG during 4 h at 37 °C. Cells were harvested by centrifugation, resuspended in lysis/wash buffer (50 mM Tris/HCl, 300 mM NaCl, pH 8.0) supplemented with 10 mM imidazole and 0.1% Triton X-100, and lysed by sonication with a Vibra Cell apparatus (Bioblock Scientific), 3 times

30 s (microtip 4, 50% duty cycle) in ice. After centrifugation at $30,000 \times g$ for 30 min, the supernatant was loaded into a preequilibrated 10-ml Nickel Chelating Fast Flow column (Amersham Bioscience) connected to an ÄKTA purifier (GE Healthcare). After extensive washing with the wash buffer supplemented with 10 mM imidazole, a 10-column volume linear gradient of imidazole (up to 300 mM) in the same buffer was applied. Fractions containing high concentrations of pure protein were identified by SDS-PAGE, pooled, concentrated by ultrafiltration (Vivaspin, 10kDa) to about 5 mg/ml in 10 mM Tris/HCl buffer, 150 mM NaCl, 2.5 mM CaCl₂, pH 8.4. The His₆-tag was cleaved by thrombin digestion (1 UE for 2 mg of protein, Novagen) at 12 °C for 2 h and the reaction stopped with 2 mM PMSF. The residual tagged protein was removed by elution through a nickel-affinity column with the wash buffer plus 10 mM imidazole. The untagged protein was concentrated to 5-8 mg/ml and applied to a HiLoad 16/60 Superdex 75 column (Amersham Biosciences) using 20 mM Tris/HCl, 50 mM NaCl, pH 8.0 as elution buffer. Enzymes/domains were either used immediately after purification or stored at -20°C in buffer supplemented with 50% (v/v) glycerol.

TLC analyses

The standards used for TLC analyses were acquired as follows: the racemic mixture of C₃₂ mycolic acid methyl esters and the C₃₁ long chain ketone and long chain alcohol were a generous gift of Dr. C. Asselineau and Prof. J. Asselineau (Asselineau and Asselineau, 1966); the TMM, TDM and GMM were isolated from *C. glutamicum* as described (Tropis et al., 2005); the diC₁₆-Tre and C₁₆-Glc were a generous gift of Prof. J.F. Tocanne (Tocanne, 1975); the C₁₆-Gro was purchased from Sigma-Aldrich (product # M1640), [1-¹⁴C]C₁₄ acid was from American Radiolabeled Chemicals (product # ARC 0198), [1-¹⁴C]C₁₆ acid and [1-¹⁴C]C₁₆-CoA were from PerkinElmer (product # NEC075H and NEC5550, respectively). Cold standards were revealed by spraying with 0.01% (w/v) rhodamine B in 0.25 M NaH₂PO₄:ethanol, 9:1 and UV light (254 nm) or 0.2% (w/v) anthrone in concentrated H₂SO₄ followed by heating.

MALDI-TOF MS and MS/MS

The condensation products were extracted from cold reaction media using a $\text{CHCl}_3/\text{CH}_3\text{OH}/\text{H}_2\text{O}$, 8/4/3 mixture, dried and dissolved in CHCl_3 before spotting. MS and MS/MS analyses were performed using the 5800 MALDI-TOF/TOF Analyzer (Applied Biosystems/ABSciex). Ionization was achieved by irradiation with a Nd:YAG laser (349 nm) and MALDI-TOF mass spectra were acquired in reflectron positive mode. For MS analysis, mass spectra were the sum of 1500 laser shots. For MS/MS analysis, a collision energy of 1 keV with air as the collision gas was used to induce fragmentation, with an accumulation of 2500 laser shots for each spectrum. Lipid standards were used to calibrate the mass spectrometer.

Homology modeling, structural comparison and visualization

The SWISS-MODEL program (www.swissmodel.expasy.org) (Arnold et al., 2006) was used to generate a homology model from the sequence of TE_{Pks13} domain. In the Automated mode, the structure of TE_{hFAS} domain in complex with methyl γ -linolenylfluorophosphate (PDB-3TJM) (Zhang et al., 2011) was selected as the best template by the program. The generated model comprises residues 1443-1717 of Pks13 that correspond to residues 2219-2499 of hFAS, leading to 18% identity (32% similarity) for 94% sequence coverage. The stereochemical quality of the model was verified with the program PROCHECK (Laskowski et al., 1993), indicating that 98% of the residues were in allowed regions of a Ramachandran plot, compared to 100% for the 3TJM template structure, and only few residues were highlighted because of distorted geometry. Model quality was also estimated using the QMEAN server (Benkert et al., 2009) that computes a composite QMEAN scoring function (ranging from 0 to 1, with higher values corresponding to more reliable models), which is a linear combination of six structural terms. Values obtained for the PDB-3TJM structure and the TE_{Pks13} domain were 0.77 and 0.51, respectively. Other

modelling schemes performed using other templates and structure-based alignments computed using the DaliLite program (Holm and Park, 2000) at the EMBL-EBI Web Server (<http://www.ebi.ac.uk/>), were not satisfactory in terms of both sequence coverage and modelling statistics. For instance, the QMEAN scores obtained for discarded models ranged from 0.22 to 0.41. Structure visualization and analyses were carried out using the PyMOL program (www.pymol.org).

SUPPLEMENTAL REFERENCES

Ahibo-Coffy, A., Aurelle, H., Lacave, C., Prome, J. C., Puzo, G., and Savagnac, A. (1978). Isolation, structural studies and chemical synthesis of a 'palmitone lipid' from *Corynebacterium diphtheriae*. *Chem. Phys. Lipids* 22, 185-195.

Asselineau, C., and Asselineau, J. (1966). [Stereochemistry of the corynomycolic acid]. *Bulletin de la Societe chimique de France* 6, 1992-1999.

Benkert, P., Kunzli, M., and Schwede, T. (2009). QMEAN server for protein model quality estimation. *Nucleic Acids Res.* 37, W510-514.

Holm, L., and Park, J. (2000). DaliLite workbench for protein structure comparison. *Bioinformatics* 16, 566-567.

Laskowski, R.A., Macarthur, M.W., Moss, D.S., and Thornton, J.M. (1993). Procheck - a Program to Check the Stereochemical Quality of Protein Structures. *J. Appl. Crystallogr.* 26, 283-291.

Tocanne, J.F. (1975). [A new synthesis of cord factor, the toxic glycolipid from *Mycobacterium tuberculosis*. (Trehalose and alpha-branched, beta-hydroxylated fatty acid esters)]. *Carbohydrate research* 44, 301-307.

Weiner, M.P., Costa, G.L., Schoettlin, W., Cline, J., Mathur, E., and Bauer, J.C. (1994). Site-directed mutagenesis of double-stranded DNA by the polymerase chain reaction. *Gene* 151, 119-123.